2017•2018
Faculteit Industriële ingenieurswetenschappen
master in de industriële wetenschappen: elektronica-ICT

Masterthesis

A study on the state of the art of conductive silicone nanocomposites for stretchable electronics

PROMOTOR :
Prof. dr. ir. Wim DEFERME

COPROMOTOR :
ing. Steven NAGELS

Jeff Rutten

Scriptie ingediend tot het behalen van de graad van master in de industriële wetenschappen: elektronica-ICT

Universiteit Hasselt | Campus Diepenbeek | Agoralaan Gebouw D | BE-3590 Diepenbeek
Universiteit Hasselt | Campus Hasselt | Martelarenlaan 42 | BE-3500 Hasselt

2017 • 2018

Faculteit Industriële ingenieurswetenschappen

master in de industriële wetenschappen: elektronica-ICT

Masterthesis

A study on the state of the art of conductive silicone nanocomposites for stretchable electronics

PROMOTOR :
Prof. dr. ir. Wim DEFERME

COPROMOTOR :
ing. Steven NAGELS

Jeff Rutten

Scriptie ingediend tot het behalen van de graad van master in de industriële wetenschappen: elektronica-ICT

UHASSELT

KU LEUVEN

Acknowledgements

First of all, I would like to express my gratitude to both of my supervisors, Steven Nagels and Wim Deferme, for their continuous support, encouragement and guidance. If I had questions or remarks, their office doors were always open. A special shout out is required for Steven, whose enthusiasm and energy were infectious and his effort for manufacturing the powder press greatly appreciated.

Furthermore, I would like to thank the researchers of Chem & Tech for their hospitality. A special shout out goes to Roberta, Anja and Steffen for supporting me during the experiments. Without the use of their three roll mill and high speed mixer, the results of this thesis were otherwise unobtainable.

In addition, I would like to thank the other researchers at IMO-IMOMEC for the various amusing moments and guidance throughout the year.

Finally, I would like to thank my parents and sister for supporting me throughout my studies. A special thanks goes out to my girlfriend whose kindness and motivations kept me going during this thesis.

Table of Contents

List of tables

List of figures

Abstract

One of the topics at IMO-IMOMEC of Hasselt University is the investigation of stretchable electronics by designing conductive composites, consisting of PDMS and conductive fillers. However, the percolation thresholds of these fillers are still unknown and scientifically accurate measurements are required, since high filler concentrations past the percolation threshold will aggravate the mechanical characteristics of the nanocomposite. During this Master's thesis, the percolation threshold of 7 conductive fillers is explored.

In order to determine the percolation thresholds, multiple dispersion techniques are investigated, including ball milling, three roll milling, solution mixing and high speed mixing. Afterwards, the percolation threshold of the fillers is investigated by fabricating multiple samples at specific filler weight percentages and by measuring the resistance of each sample. Finally, the composites are characterized to determine the maximum elongation until the loss of conductivity occurs.

The experiments show that three roll milling and high speed mixing yields the best dispersion. Furthermore, the percolation threshold decreases as the aspect ratio of the used filler increases. Finally, the composites containing spherical particles such as carbon black are suitable for strain sensor applications due to the higher gauge factor. On the other hand, multi-walled carbon nanotube composites exhibit favorable properties for stretchable conductors since the resistance remains almost constant during an elongation of 100%.

Samenvatting

Een van de vele research topics binnen IMO-IMOMEC van de universiteit Hasselt is het onderzoek naar rekbare elektronica door gebruik te maken van geleidende composieten, bestaande uit PDMS en geleidende *fillers*. The percolatie grenzen van deze *fillers* zijn echter niet gekend and wetenschappelijke nauwkeurige metingen zijn nodig omdat een te veel aan geleidende *filler* de mechanische eigenschappen van de composiet schaadt. Tijdens deze master thesis warden de percolatie grenzen van 7 verschillende *fillers* onderzocht.

Voor de percolatie grenzen te onderzoeken zijn er meerde dispersie technieken onderzocht, namelijk *ball milling, three roll milling, solution mixing* en *high speed mixing*. Daarna zijn de grenzen onderzocht door verschillende *samples* te maken met een specifiek gewichtspercentage aan filler en overeenkomstige weerstand is gemeten. Ten slotte zijn de *samples* gekarakteriseerd op basis van maximale rek tot breuk.

De experimenten tonen aan dat *three roll milling* en *high speed mixing* de beste dispersie geven. De percolatie grenzen verlagen naarmate de *aspect ratio* van de *filler* toeneemt. Ten slotte de composieten met ronde *fillers* zijn geschikt voor een rek sensor door de grotere *gauge factor*. De composieten met *multi-walled carbon nanotubes* hebben geode eigenschappen voor rekbare geleiders aangezien hun weerstand tijdens rek tot 100% nagenoeg constant blijft.

Introduction

The introductory chapter of this thesis will give an outline of the background, problem definition and research question, as well as the objectives of this thesis. Furthermore, the following paragraphs will describe the used methodology in order to resolve the encountered problems.

Background

This Master's thesis is located within the Functional Materials Engineering (FME) research group at IMO-IMOMEC, a research facility of the Hasselt University which is specialized in innovative materials. FME is mainly engaged in the development of functional materials and its research domain can be divided in three prominent clusters, namely the printability, deposition and application of functional materials. Situated within these clusters, FME investigates stretchable electronic conductors which will be incorporated into stretchable circuits in the future.

The demand for stretchable electronics has risen significantly in recent years. Zion Market Research, a market research company which delivers cutting edge industry reports, expects that the market will be valued at 16.50 billion dollars by the end of 2021 [1]. The global market for stretchable electronics include various fields such as automotive engineering, textiles, aerospace, telecommunication and most importantly, health care. Healthcare is the expected prominent field in which stretchable electronics will lead to numerous innovations such as monitoring the nerve activity during spinal surgery, patches that are able to measure the amount of sun exposure and assisting neuroscience research, where devices radiate light in order to further explore and map the brain [2].

Problem definition and research question

Stretchable electronics have various benefits such as being thin, light and improving the reliability of applications which are subjected to a lot of stress . These characteristics are useful for numerous applications such as stretchable display, wearable health systems, soft robotics, etc. This requires conductive and stretchable materials, which can withstand large amounts of stress and deformations while maintaining the conductivity of the material. For intrinsically conductive and stretchable materials, the chemical bonds will elongate microscale wise during stretching, leading to delocalized orbitals. This results in an increased electrical resistance or macroscale cracks in the material [3].

Currently, the literature already reports multiple methods for developing stretchable conductors. The first method is the implantation of conductive fillers into the

surface of an elastomer. Secondly, microchannels are engraved within the elastomer by utilizing soft lithography and these microchannels are filled with a liquid metal. The third method consists of the in situ synthetization of metal particles within the elastomer. Furthermore, elastomers can infiltrate networks of conductive fillers. The last method involves mixing conductive fillers with elastomers in order to achieve conductive composites [4].

The production method of choice for a conductor in this research is the blend of an elastomer with conductive fillers. By gradually increasing the amount of fillers in the blend, the resistance will drop significantly past a certain volume percentage. In literature, this volume percentage is known as the percolation threshold. When the percolation threshold is reached, the composite transforms into a conductor because a conductive path is formed within the polymer due to the entanglement of conductive filler particles.

Currently, IMO-IMOMEC has a limited amount of blends and multiple conductive fillers need to be examined. Previous work [3] already laid the foundation of this thesis but the obtained percolation thresholds and the corresponding resistances were only an exploration of the possibilities, scientifically accurate measurements still need to done, which will be performed in this thesis. This results in the following research question:

"What are the various percolation thresholds of the examined conductive fillers in a PDMS matrix, and which filler exhibits the highest sensitivity towards pressure or temperature changes, in order to select the most sensitive composites for the manufacturing of a soft sensor"

Objectives

In this thesis, electronic conductors for stretchable circuits and sensors are investigated. The main goal of this research is the development of stretchable interconnects which can be used for stretchable electronics. Currently, no external power source can be attached to the developed stretchable circuits because the interconnects are fabricated using a liquid metal, so the circuit has to be self-sustainable by incorporating an energy source like a battery. By using the solid and stretchable interconnects which are developed in this thesis, the liquid metal can be encapsulated and prototyping of stretchable electronics will be facilitated.

The first goal of this research is to determine the best dispersion method for mixing the fillers and PDMS in order to obtain a homogenous blend is.

The second goal consists of the development of a stretchable conductor by mixing an elastomer with various conductive fillers and determining the various percolation thresholds and their corresponding resistance. In order to ensure the conductivity of the used materials, a device is made to measure the resistivity of the bulk powders.

The final goal is the characterization of the composites, in order to determine which kind of sensor can be made with the composite. The type of sensor is still unknown since it is dependent on the characteristics of the conductive composite such as the sensitivity towards pressure and temperature changes. For instance, when the composite exhibits high sensitivity towards pressure changes, the composite will be used for the manufacturing of a soft pressure sensor, instead of a temperature sensor.

Materials and methods

Each polymer blend in this paper includes conductive particles and elastomers. The most prominent silicone elastomer is polydimethylsiloxane. PDMS has outstanding properties such as thermal stability, transparency, chemical inertness and viscoelasticity. It is obtained by a polymerization reaction between dimethyldichlorosilane and water. The different fillers discussed in this thesis include multi-walled and two types of single-walled carbon nanotubes, carbon black, a mixture of carbon black and carbon nanotubes, silver nanowires and silver coated copper flakes. Each filler enhances the characteristics of the blend in a unique way, such as the viscosity and conductivity.

Firstly, multi-walled carbon nanotubes consist of numerous concentric graphene cylinders with various diameters. They exhibit exceptional thermal, electrical and mechanical characteristics, thus making MWCNT one of the most intriguing candidates for conductive fillers in polymer nanocomposites [5]. Furthermore, single-walled carbon nanotubes consist of a single cylindrical graphene cylinder. The thermal, electrical and mechanical characteristics of SWCNTs are comparable to MWCNTs, whereby MWCNTs have a slightly higher Young's modulus [6].

Carbon black is obtained by an incomplete combustion of carbonaceous materials. It is a fine mixture of individual dried carbon particles [7]. The mixture of carbon black and carbon nanotubes has an unknown mixing ratio. Since carbon black is made out of carbon, carbon black acts as a semiconductor.

Silver nanowires are exceptional for use as a conductive filler because silver has the highest conductivity of all metals. Thanks to the shape of the nanowires, conductive paths are created faster and easier between the filaments so a lower volume percentage is required in order to achieve electrical conductivity when compared with silver powder [8].

And finally, silver coated copper flakes provide a budget friendly alternative to pure silver powder since a silver coating is applied to a copper nucleus [9].

However, it is important to remark that the fillers, predominantly the metal powders, could contain contaminations, so its recommended to clean the fillers in

order to achieve maximum purity, since these contaminations will affect the measurements.

For the first part of this thesis, namely the investigation of the optimal dispersion method, various fillers will be mixed through the PDMS and the resulting samples are compared to each other.

The second part of this thesis consists of the percolation threshold measurements where each conductive filler will be dispersed within the PDMS and cured into sample. Each filler starts at a known weight percentage, and the weight percentage is increased gradually with each step. The percolation threshold is reached when the resistance drops significantly. This approach was chosen because the method of the previous work [3] wasn't accurate enough. It used a round bottom flask which had tungsten electrodes attached through the bottom, while a four-wire measurement continuously monitored the resistance of the mixture. In order to perform the four-wire measurement, a Keithley multimeter 2000 was used. The measuring flask was not optimal because problems arise during the evaporation of the diluting agent acetone. Since the flask had a round bottom, a continuous air flow was not possible and the solvent stayed within the composite which affected the properties of the blend.

For the final part of the thesis, the composite will be characterized and the influence of external factors such as strain on the resistivity will be investigated. A blade coater is used create a homogenous layer of the composite suspension and the final composite is obtained by curing the sample.

1. Stretchable conductors: a theoretical overview

The majority of electronics that we use daily are fabricated using rigid components. While rigid electronics are still dominant within the industry, stretchable electronics are progressively gaining interest as a feasible alternative. This is due to the increasing demand of wearable displays, soft robotics, wearable healthcare devices, and stretchable batteries. Accordingly, the future of electronics is shaping towards complex multifunction circuits incorporated in clothing or on the human skin. These circuits need to be able to withstand stretching and folding to a certain degree while maintaining their performance. In order to maintain the shape of the electronics, the interconnects and substrate of the circuit need to stretchable. Researchers have developed two design approaches for stretchable electronics, namely mounting rigid components on a stretchable substrate and manufacturing stretchable components [3],[4].

Axisa et al. have demonstrated the first design approach by producing a stretchable thermometer, which consists of a resistor, led and capacitor, an embedded SMD thermometer, a power supply and a temperature sensor, all of which are rigid components [12].

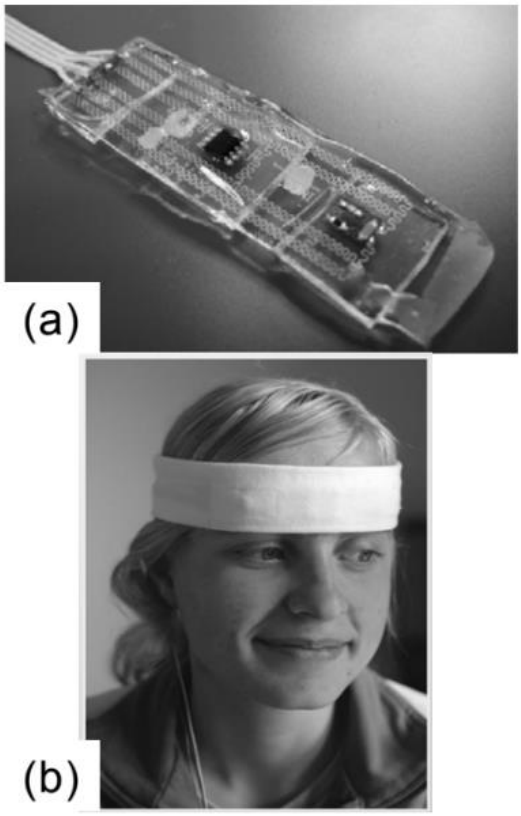

Figure 1: (a) a stretchable thermometer and (b) the thermometer embedded in a textile band [12]

The interconnects have a meander design which is the optimal design for stretchable conductors, as confirmed by Gonzalez et al. [13]. In order to test the designs, an axial deformation of 20% was applied on the meander. The crest of the ellipsoid had the highest concentration of mechanical stress and to reduce the amount of stress, a rounded shape such as the horseshoe design is preferred, as illustrated in the following figure [3].

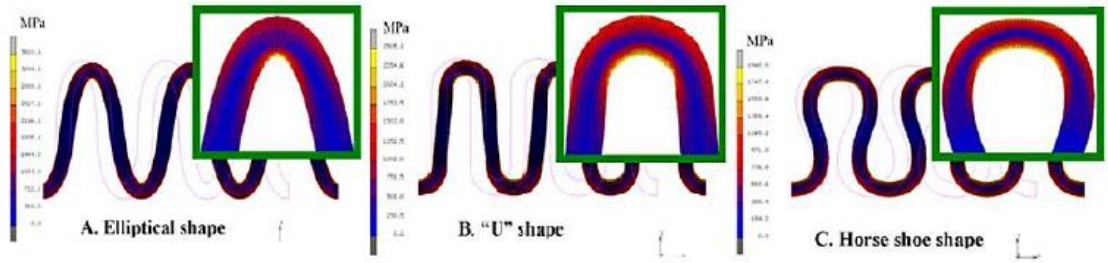

Figure 2: The distribution of stress in different conductor shapes: (a) ellipsoid, (b) "U" shape and (c) horseshoe shape [3]

The second design philosophy consists of manufacturing stretchable and conductive materials in order to make the whole circuit deformable. A promising method for achieving stretchable electrodes and circuits is the design of conductive composites, consisting of an elastomer and conductive fillers. Multiple methods for designing conductive composites are reported in the literature, including the implantation of conductive fillers into the surface of an elastomer, engraving microchannels in an elastomer, the in situ synthetization of metal particles within the elastomer, the infiltration of elastomers with conductive fillers and finally, mixing conductive fillers with elastomers in order to form a conductive blend [4]. The design of a conductive blend will be the method of choice in this thesis.

1.1 Conductive Blend

1.1.1 Introduction

Conductive polymer composites generally consist of conductive fillers which are mixed with an insulating polymer matrix. In order to achieve electrical conductivity within an insulating polymer, the amount of added conductive fillers is a critical manufacturing specification. When the filler concentration is too low, the conductivity of the blend will be too low for conducting an electrical current. At a critical filler load, the percolation threshold is achieved and the conductivity will increase drastically. When the filler concentration increases beyond this point, the excessive amount of fillers will not change the electrical conductivity in a meaningful

way. Moreover, the rheological and mechanical properties will aggravate because higher filler concentrations will result in a higher viscosity and a more brittle composite after curing. As a result, it is advised to keep the filler concentration slightly above the critical amount which is required for percolation.

Other interesting points of research for conductive composites, besides the filler concentration, are the various factors that influence the percolation threshold. The electrical properties, such as the percolation threshold and the electrical conductivity of the conductive blend are substantially modified by the dispersion state of the filler, and geometric characteristics of the fillers such as aspect ratio and shape.

1.1.2 The percolation theory

The electrical resistance of a polymer composite is generally dominated by the tunneling effect of electrons [15]. Electrons move within the conductive fillers themselves but they also move between fillers. They must overcome the energy barrier between fillers by the means of quantum tunneling. This results in a tunneling resistance. The tunneling resistance is dependent of the temperature and increases exponentially with increasing tunneling distance. The tunneling distance is the distance between two neighboring conducting fillers within the polymer matrix [16] and this distance determines the conductivity of the percolation network [17].

There are two categories of electrically conductive polymers, namely intrinsic and conductive polymer nanocomposites. The conductivity in intrinsically conductive polymers arises from the electronic structure of the polymer, such as the presence of an aromatic ring. The conductive polymer nanocomposites, which will be discussed in this thesis, gain their conductivity from the conductive fillers which are incorporated in the non-conductive polymer. At low filler concentrations, the composite has a conductivity which is approximately the same as the conductivity of the pristine polymer. The reason is that fillers are isolated within the polymer matrix below a critical filler fraction. When the volume percentage of the filler increases, the non-conductive polymer blend will transition into a conductor. At this critical filler loading, the percolation threshold, the concentration of filler particles is high enough to create a conductive structure right through the matrix of the insulating polymer, which is illustrated in the following figure [18].

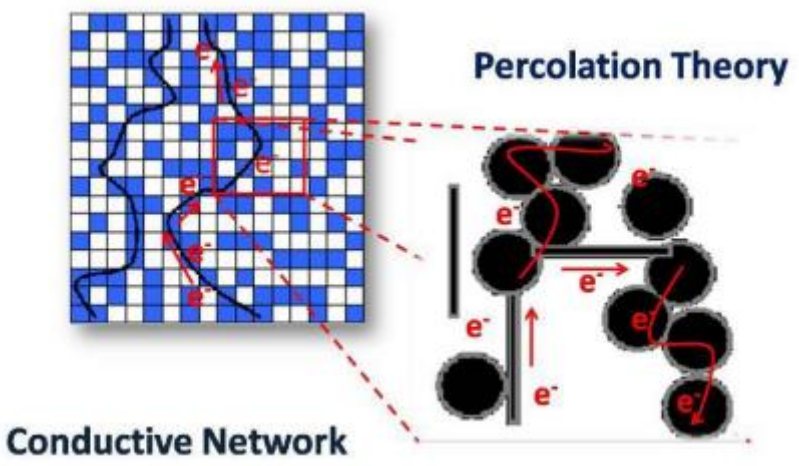

Figure 3: Percolation threshold, a conductive pathway for electrons [18]

The conductivity of the blend increases multiple orders of magnitude in this percolation zone. Once the percolation zone is passed, the changes in conductivity due to increased filler loading are minimal until the conductivity of the blend approximates the intrinsic conductivity of the bulk filler [18]. In other words, when the filler load in a composite increases, the changes in conductivity generally show a percolation curve which is S-shaped, as depicted in the following figure.

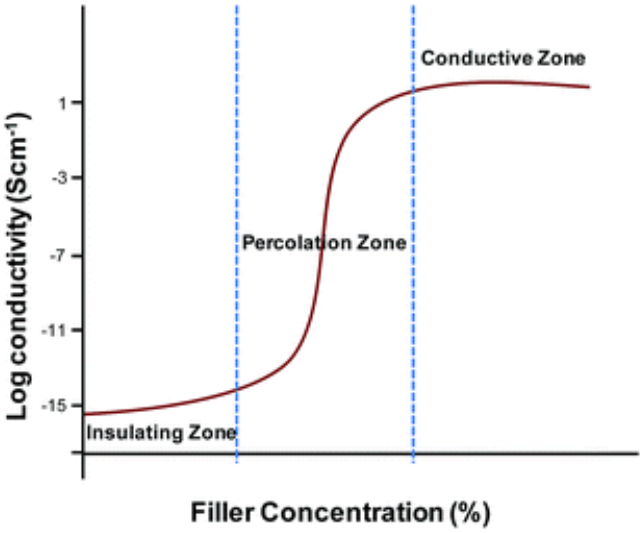

Figure 4: The conductivity of the composite as function of the amount of filler [19]

This phenomena is known as the percolation theory and at the vicinity of the threshold, the conductivity of a polymer composite follows a power law dependence [3]:

$$\sigma = \sigma_0 (V_f - V_c)^s$$

Formula 1: The power law dependence at the percolation threshold [3]

Where $\boldsymbol{\sigma}$ is the conductivity of the polymer composite, $\boldsymbol{\sigma}0$ is a proportional constant which is dependent of the conductivity of the filler, V_f is the concentration of the conductive filler, V_c is the filler concentration at the percolation threshold and S is a constant which is dependent on the structure of the composite, which is generally 2 for 3D structures and 1.33 for 2D structures. However, values of t as high as 10 have been reported but the reason maintains unknown although researchers suggest that complex tunneling transport processes within polymer composites cause this nonuniversality [14].

1.1.3 Modelling

Mathematicians and scientists have created multiple models describing the percolation phenomenon since it is based on the probability of contact and random distribution of the conductive particles within the composite. The power law dependence, as described in the previous paragraph, is a basic yet general model to describe the percolation phenomena, both numerically and analytically. However, theoretical and experimental data emphasize that the power law dependence is only valid at the vicinity of the percolation threshold, the power law model cannot characterize the insulating and conducting zone. Furthermore, only cylindrical fillers such as metal nanowires and carbon nanotubes are suitable for this model [14]. This can be related to the strong influence of the dispersion, orientation and aspect ratio of the conductive particles on the electrical conductivity [14].

Excluded volume model

One of the most regularly utilized analytical model for describing percolation is the excluded volume model. The concept of this model is that the percolation threshold of a filler in a composite is primarily dependent of the excluded volume of the conductive fillers, instead of their actual volume. "The excluded volume of an object is defined as the volume around the object into which the center of mass of another identical object cannot enter without contacting the first object" [14, p. 17], as illustrated in the following figure:

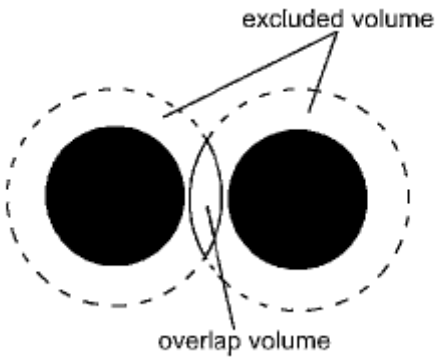

Figure 5: An illustration of the excluded volume of fillers [14]

The excluded volume model, unlike the power law dependence, can be applied to rod shaped fillers and is expanded for particles which have an aspect ratio of 100 or more. Furthermore, the excluded volume model differentiates polydispersed and monodispersed rod networks [14]. In a monodispersed network, each filler has the same dimensions without deviations while in a polydispersed network, the fillers have distinct sizes. The following equation describes the general excluded volume of a cylindrical particle, where L and D are the length and diameter of the particle, respectively [14].

$$V_{ex\_rod} = \frac{\pi}{2} D \left[\frac{\pi}{4} D^2 + L^2\right] + \frac{\pi}{4} D^2 L(3 + \pi)$$

Formula 2: The excluded volume of a cylindrical particle [14]

The excluded volume of a particle is inversely proportional with the critical amount of particles which is needed for percolation, as given by the following equation:

$$N_c \sim \frac{1}{V_{ex\_rod}}$$

Formula 3: The required amount of particles for percolation [14]

Monodispersed rod network

As mentioned in the previous paragraph, each filler in a monodispersed network has the same dimensions without deviations. However, there are multiple equations, depending on the aspect ratio of the particle [14].

For cylindrical fillers with a finite aspect ratio, the percolation threshold is described by the following equation [14]:

$$\varphi_c = N_c V_{rod} = \frac{V_{rod}}{V_{ex\_rod}} = \frac{(1 + s)\frac{\pi}{4} D^2 L}{\frac{\pi}{2} D \left[\frac{\pi}{4} D^2 + L^2\right] + \frac{\pi}{4} D^2 L(3 + \pi)}$$

Formula 4: The percolation threshold for cylindrical fillers with a finite aspect ratio in a monodispersed rod network [14]

Where V_{rod} is the actual volume of the filler, D and L the diameter and length of the filler, respectively and S is a correction factor which is determined empirically. The general equation for S is given by [14]:

$$s = 3{,}2\left(\frac{R}{L}\right)^{0{,}46}$$

Formula 5: The correction factor [14]

Berhan and Sastly [20] determined a different expression which is in accordance with the general equation of Mutiso [14], namely :

$$s = 5{,}23\left(\frac{L}{R}\right)^{-0{,}57}$$

Formula 6: An alternative correction factor [14]

Formula 4 anticipates a decrease of the percolation threshold when the aspect ratio of the rod increases, which is observed in simulations along with experiments [14],[18].

In case of particles with an infinite aspect ratio (L/D -> ∞), the percolation threshold is determined as follows [14]:

$$\varphi_c = \frac{V_{rod}}{V_{ex\_rod}} = \frac{\frac{\pi}{4}D^2L}{\frac{\pi}{2}D\left[\frac{\pi}{4}D^2 + L^2\right] + \frac{\pi}{4}D^2L(3+\pi)} = \frac{1}{\frac{\pi}{2}\frac{D}{L} + 2\frac{L}{D}(3+\pi)}$$

Formula 7: The percolation threshold for cylindrical particles with an infinite aspect ratio in a monodispersed rod network [14]

Polydispersed rod network

In contrary to a monodispersed rod network, the size of the particles is inconsistent, hence the presence of a normal distribution in particle size. Under these circumstances, the percolation threshold can be described by the following equation [14]:

$$\varphi_c = \frac{(1+s_{poly})\frac{\pi}{4}D_n{}^2L_n}{\frac{\pi}{2}D_n\left[\frac{\pi}{4}D_n{}^2 + L_n{}^2\right] + \frac{\pi}{4}D_n{}^2L_n(3+\pi)} = \frac{(1+s_{poly})}{\frac{\pi}{2}\frac{D_n}{L_n} + 2\frac{L_n}{D_n}(3+\pi)}$$

Formula 8: The percolation threshold for cylindrical particles in a polydispersed rod network [14]

Where L_n and D_n are the average length and diameter of the cylindrical filler, respectively and S_{poly} the empirical correction factor, which is given by [14]:

$$s_{poly} = 3{,}2\left(\frac{D_n/2}{L_n}\right)^{0{,}46}$$

Formula 9: Correction factor [14]

A percolation model for spherical particles

The previous described percolation models relate to cylindrical particles. In order to model spherical granulates, like carbon black and metal powders, Bruggeman et al. developed the effective media theory. The effective media approximation considers a binary medium which is inhomogeneous on the macroscopic scale, whereby material properties such as the conductivity vary in space. A binary composite, such as randomly dispersed spherical granulates within a polymer matrix, can be modelled using this approximation. The effective conductivity of the composite $\boldsymbol{\sigma}$M can be calculated when the intrinsic conductivity and volume fraction of the spherical particles and polymer matrix are known [3],[21]:

$$\varphi_L\left(\frac{\sigma_L - \sigma_M}{\sigma_L + 2\sigma_M}\right) + \varphi_H\left(\frac{\sigma_H - \sigma_M}{\sigma_H + 2\sigma_M}\right) = 0$$

Formula 10: The effective conductivity of the composite [21]

Where $\boldsymbol{\varphi}_H$ and $\boldsymbol{\varphi}_L$ are volume fraction of the particles and polymer matrix, respectively. $\boldsymbol{\sigma}_H$ and $\boldsymbol{\sigma}_L$ are the conductivity of the particles and polymer matrix, respectively and $\boldsymbol{\sigma}_M$ is effective conductivity of the composite.

1.2 Factors that affect the conduction behavior of the composite

The conductivity of the blend is greatly affected by multiple factors such as the concentration, the geometry and the intrinsic conductivity of the filler [18]. Finally, the dispersion state is one of the most influential factors and will be discussed in a separate paragraph.

1.2.1 Filler concentration

When the concentration of the filler is to low, the presence of the filler in the composite will hardly reduce the resistivity of the blend, as depicted in figure 2. At concentrations below the percolation threshold, the quantity of conductive filler is too small in order to create a conductive pathway. Very few particles are nearby or even in contact with each other, which results in many gaps of considerable size between the fillers. These gaps increase the tunneling resistance and thus the resistance of the blend [18].

At the percolation threshold, the amount of contacts between particles increases precipitously and the conductive particles are now either &separated by miniscule gaps or actually in contact with each other, resulting in a conductive path. Further increment of the filler concentration will increase the amount of parallel conductive paths and the resistance of the blend will decrease accordingly [18].

1.2.2 Intrinsic conductivity of the filler

The electrical resistance of the blend is influenced by the intrinsic resistance of the matrix and filler, and the interaction between the polymer and fillers. Fillers with a high intrinsic conductivity yield better conducting composites. Thus fillers such as metallic particles, which are known for their high volume conductivity, will outperform nonmetallic fillers like carbon black regarding electrical conductivity when used in a composite.

Besides the electrical properties of the filler, the bonding between conductive particles and polymer matrix will greatly influence the blend. A high filler-polymer bond results in a thick coating of the polymer around the filler which obstructs the interaction between conductive particles, contributing to the lower conductivity of the composite [18].

1.2.3 Geometry of the filler

The critical concentration for a given filler is dependent on the attributes of the filler, such as the aspect ratio (L/D). For instance, a spherical particle has an aspect ratio of 1 and a cylindrical stick has an aspect ratio which is equivalent to the ratio of its length to its diameter. The percolation threshold decreases when the aspect ratio increases, as illustrated in the following figure [18]:

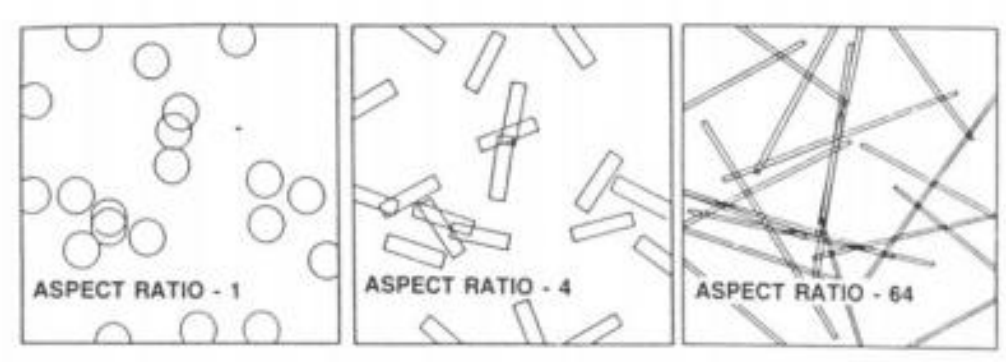

Figure 6: An increased aspect ratio lowers the percolation threshold [18]

In each frame of figure 6, the orientation and the occupied area of the filler remains unchanged but the aspect ratio varies between 1 and 64 [18]. Both theoretical and experimental studies confirmed the strong influence of the aspect ratio of the conductive filler on the conductivity of the composite, whereby high conductivity and low percolation thresholds are achieved by utilizing high aspect ratio fillers.

Rosca et al. found that the conductivity of the composite increased 10 times as the aspect ratio of the fillers increased 5,5 times [38]. The impeccable performance of high L/D fillers is due to their efficiency to create networks which require fewer physical contacts, resulting in percolation thresholds as low as 1 vol% for carbon nanotube composites [14]. In comparison with more conventional fillers, the spherical carbon black has a typical percolation threshold around 15 wt% and metallic powders, such as copper and silver, have thresholds as high as 60 wt% [14]. When the aspect ratio of the conductive filler changes, the classic S-shaped percolation curve is maintained. However, when the aspect ratio increases, the formation of the conductive path will occur at lower filler quantities [18].

The size of the filler will also affect percolation, especially when combining different fillers. The following figure illustrates the effect of combining two spherical fillers, with R1 and R2 being the size of the major and minor filler, respectively. The smaller sized particles are forced between into various gaps between the bigger sized particles, resulting in more contacts and thus higher conductivity [11].

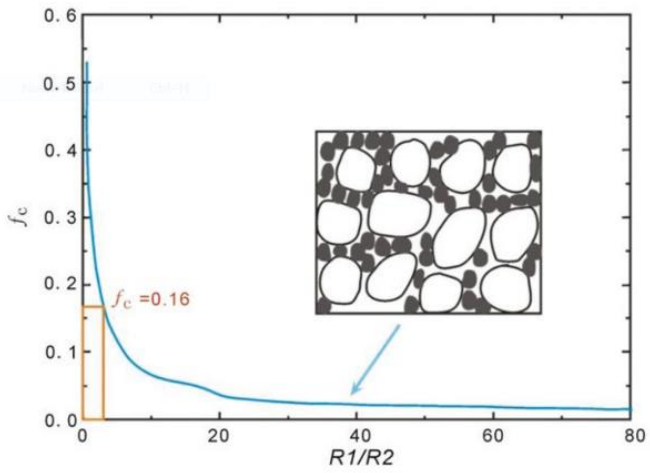

Figure 7: The percolation threshold decreases when the ratio of the filler sizes increases [11]

In case of composites which are filled with only one kind of filler, Xue et al. concluded that the percolation threshold for metal -polymer composites increased as the particle size of the filler increased [12], as illustrated in the following figure [25]:

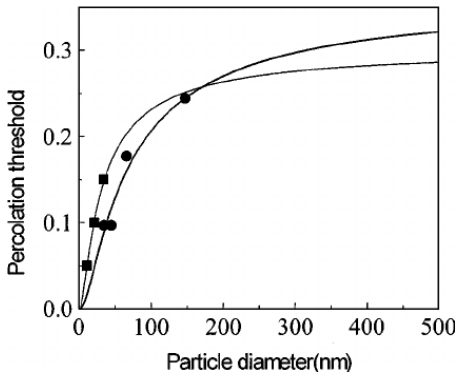

Figure 8: The percolation threshold increases with increased filler size, where the solid circles and solid squares represent data taken from the references [25]

1.2.4 Orientation of the filler within the network

The orientation of the filler has a notable influence on percolation, especially for anisotropic particles like metal nanowires and carbon nanotubes. Shear forces during the processing of the composite can align anisotropic fillers within a polymer but when rod-shaped fillers become too aligned, the amount of contacts between fillers and thus the conductivity will decrease [26]. Kalaitzidou et al. [26] investigated this phenomena by comparing injection molding and compression molding. Compression molding yields the lowest percolation threshold due to the random orientation of the fillers within the polymer. Injection molding aligns the fillers along the flow direction, resulting in fewer contacts between fillers, as illustrated in the following figure [26]:

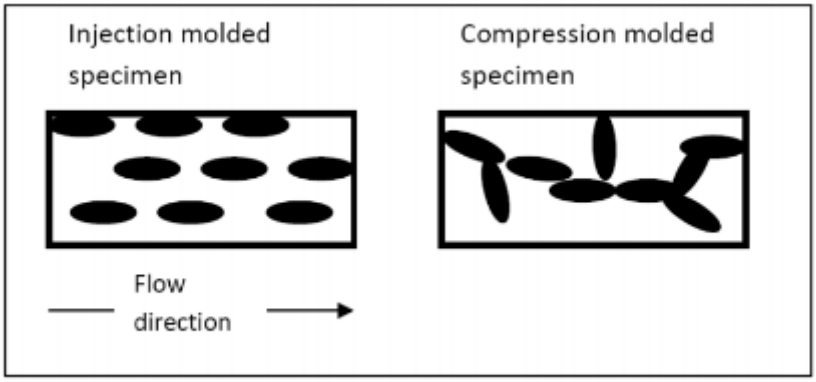

Figure 9: The alignment of the fillers affect the percolation threshold [26]

1.3 The dispersion state of fillers

In most experimental and theoretical studies of conductive polymer composites, a homogenous dispersion state of the filler within the polymer matrix is assumed. Nanoscopic particles however have the intention to form agglomerates in polymers due to their notable Van der Waals forces. Commonly used particles which exhibit strong Van der Waals forces are graphene carbon nanotubes and silver nanowires.

The complicated entanglement as a result of Van der Waals forces and the inertness of the particles are the obstacles for exploiting these fillers successfully. In order to disperse the particles homogenously, the interparticle forces have to be overcome. The dispersion of the fillers is an important parameter for manipulating the electrical characteristics of the conductive composite [23]. Multiple dispersion techniques are investigated in this thesis, each with their respective advantages and disadvantages, such as solution mixing, ball milling, manual mixing, three roll milling and dual asymmetric centrifugation.

1.3.1 Solution mixing

Solution mixing is a process of mixing a polymer and fillers in diluted state. It generally consists of three distinctive steps, namely (1) obtaining a stable suspension by dispersing the nanoparticles in an appropriate solvent, (2) mixing the polymer with the stable filler suspension and (3) obtaining the final composite by evaporating the remaining solvent. Generally, the fillers and polymer are dispersed in a common solvent. However, most conductive particles, especially carbon based particles have large surface areas and nonpolar surfaces and as a result, they have poor dispersion in organic solvents. For that reason, carbon based particles such as graphene and carbon nanotubes are easily agglomerated and require high power dispersion tools.

In order to create a stable and well dispersed suspension, a sonicator is commonly used [27]-[34]. Sonication gives rise to shear stress by cavitation and once the cavitation bubbles in the fluid collapse, a high strain rate is created in the area around the implosion of the bubble, resulting in the shear breakage of agglomerates [35].

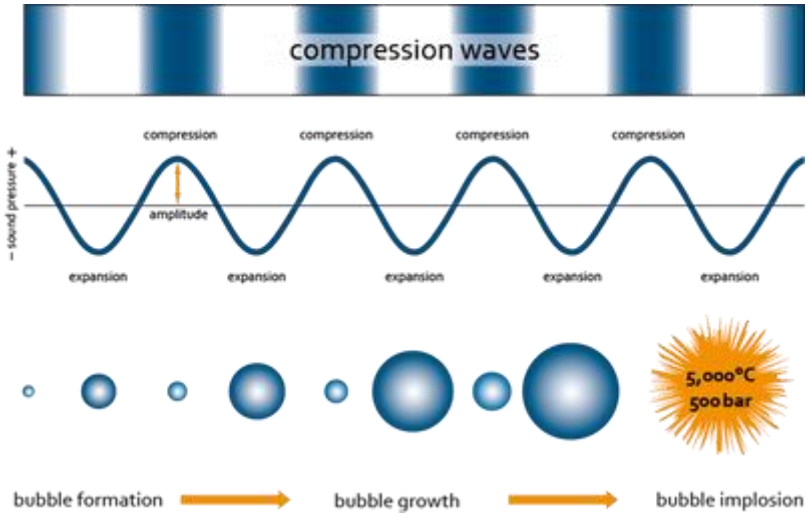

Figure 10: An illustration of the working principle of sonication [36]

Factors that affect the sonication quality include the used ultrasound frequency and intensity, the geometry of the container, the duration and intervals of the pulses and finally the external pressure and temperature. Dumée et al. investigated the effect of

the temperature during sonication and concluded that a more stable and homogenous dispersion is obtained by sonicating at a lower temperature [37]. At lower temperatures, the Van der Waals energy between particles is decreased and the re-agglomeration of the particles is slowed due to the higher viscosity of the suspension [37].

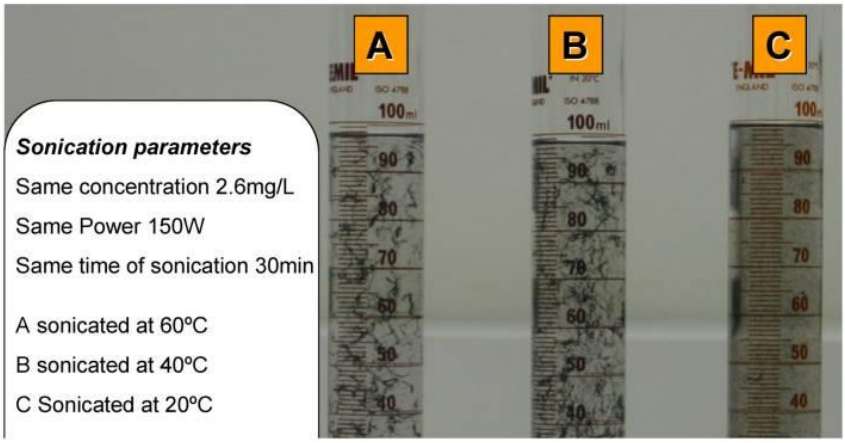

Figure 11: The effect of temperature during sonication for a carbon nanotube/IPA suspension [37]

Zheng et al. manufactured conductive carbon black and multi-walled carbon nanotube nanocomposites by utilizing the solution mixing method. The particles were first dispersed in xylene and the mixture sonicated for 20 minutes. Afterwards, the suspension was stirred by a magnetic stirrer for 1 hour and simultaneously, the PDMS, which was diluted with xylene with a volume ratio of 1:1, was also stirred for 1 hour. After an hour, the filler suspension and diluted PDMS are mixed and stirred for an additional hour. The curing agent is added by using a 10:1 mass ratio of base polymer : curing agent and suspension is stirred for 30 min. The resulting mixture is degassed and left overnight at room temperature in order to evaporate the xylene. The final composite was obtained after curing the mixture for 30 min at 100 °C [27].

The used solvent during solution mixing is an important factor which affects the dispersion state of the fillers. Xuan Liu et al. investigated the influence of common organic solvents on multi-walled carbon nanotubes nanocomposites, including toluene, chloroform, tetrahydrofuran (THF) and dimethylformamide (DMF). Out of these solvents, chloroform yielded the most stable and thus highest dispersed suspension while toluene was the least usable solvent for solution mixing [30]. Ramalingame et al. explored an additional solvent, namely isopropanol, besides the strong organic solvents like chloroform, THF and toluene. Isopropanol yielded the best dispersion stability and quality while toluene had poor dispersion quality. A proportional relationship is shown between the quality of the suspension and the pressure sensing range of MWCNT pressure sensors [29].

1.3.2 Ball milling

In contrast with solution mixing, ball milling is a dry dispersion method without the use of any solvent, which has the undeniable advantages of avoiding unhealthy and expensive solvents. Ball milling utilizes a batch reactor which contains the materials and milling tools such as zirconia balls. When the reactor moves, the milling balls inside the reactor gain kinetic energy and collisions start to occur. A small amount of material is pulverized between colliding milling balls during collisions and the material experiences mechanical load, as illustrated in the following figure [38]:

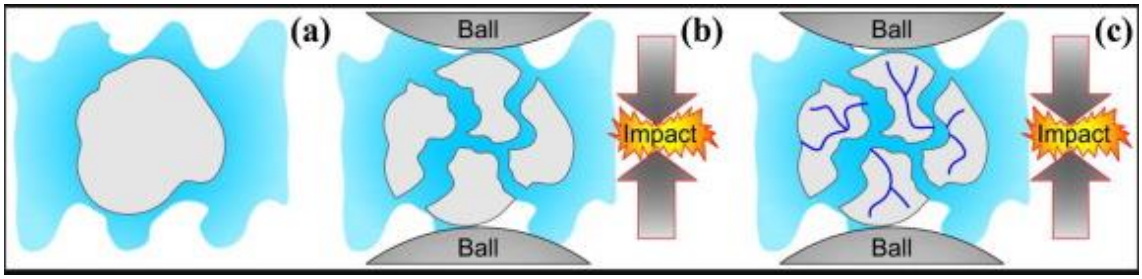

Figure 12: The impact event during ball milling: a certain amount of material (a) is crushed between colliding milling tools (b) and the repeated shattering of the material results in new deformation paths and fractures [38]

Tan et al. and Witt et al. reported conductive nanocomposites, filled with a mixture of carbon black and carbon nanotubes. Ball milling was the dispersion method of choice and the same procedure was used in both papers. Firstly, each component of the two-component silicone was mixed separately with a filler blend of carbon black and carbon nanotubes. The suspensions were mixed at a low intensity for 24 hours at 240 RPM in order to avoid any damage to the filler particles. Afterwards, the two suspensions were mixed, degassed and cured for 2 hours at 70°C. Due to the good dispersion and creation of conductive pathways, the composites had a high conductivity and exhibited great sensitivity for compressive and tensile stress [39][40].

It is reported that ball milling can reduce the aspect ratio of particles such as carbon nanotubes [33]. Pierard et al. [41] investigated the effect of vibrational ball milling on single-walled carbon nanotubes and concluded that the optimal time of ball milling is 2 hours at 3000 vibrations/minute. No notable destruction of the carbon nanotubes is observed during the first 3 hours of treatment but as the milling time increased further, the milling progressively disrupted the nanotubes. After 50 hours of milling, the structure of the carbon nanotubes eventually transformed into amorphous carbon [41].

1.3.3 Manual mixing

Manual stirring is a cheap dispersion method but it doesn't provide the required energy in order to pulverize small agglomerations [42]. Ruhhammer et al. produced

a conductive silicone by mixing silver powder into PDMS. Firstly, component A and component B of the base polymer are mixed and afterwards, the silver particles are added and the suspension is mixed by hand until a crumbly mixture is obtained. The final step consists of grinding the mixture on a glass plate with a spatula until the mixture has a smooth and homogenous appearance [31]. Stassi et al. obtained a conductive blend by gently mixing copper powder into PDMS because rougher mixing techniques could damage the tips on the surfaces of the particles [32]. During the literature review of manual mixing, it was remarkable that all the used particles had a size of a few micrometers. This could be explained by the fact that the possibility of agglomerates increases as the filler size decreases because the amount of potential energy due to repulsive forces between fillers decreases. Consequently, the Van der Waals force is the dominating force for fillers smaller than 1 micrometer [45] and during manual mixing, not enough energy is provided to overcome the strong Van der Waals forces between particles.

1.3.4 Three roll mill

Three roll milling is a technique that utilizes both extensional and shear flow in order to disperse particles into viscous materials. The high shear forces are created by three rolls which rotate at a different speed and in the opposite direction of the adjacent roll. The gap size between the rolls can be adjusted hydraulically or mechanically.

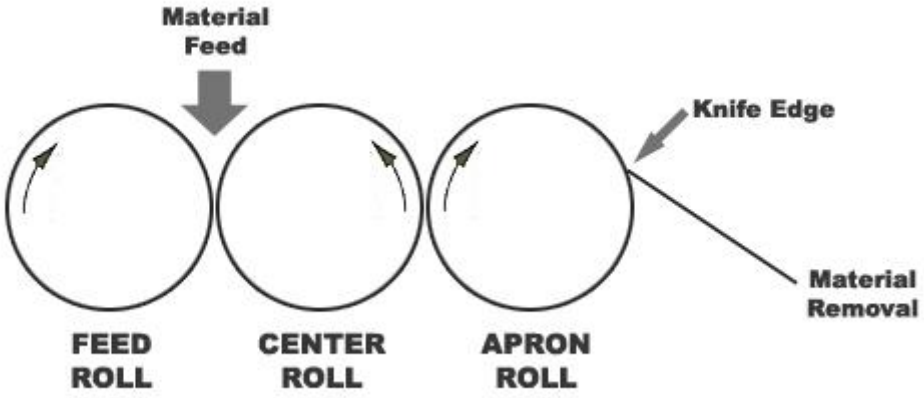

Figure 13: Schematic of a three roll mill [46]

As illustrated in figure 13, the suspension is loaded between the feed roll and the center roll. The suspension will be squeezed through the narrow nip between the rolls, resulting in powerful shear forces. The remaining suspension is transported towards the gap between the center roll and apron roll where it will experience even greater shear forces due to the progressively higher speeds of the rolls. A blade automatically scrapes the processed mixture of the apron roll and the milling cycle can be repeated until the required particle size and homogenous blend is obtained

[47]. In the literature, the three roll mill is successfully used for the fabrication of conductive MWCNT/silicone composites [22].

1.3.5 Dual asymmetric centrifugation

Dual asymmetric centrifugation or DAC is a type of speed mixer for grinding, dispersing and mixing any combination of pastes, powders and liquids. A container is rotating around a central axis but unlike a normal centrifuge, the container itself is rotating in the opposite direction, as illustrated in the following figure. These opposite movements create high shear forces within the sample [42].

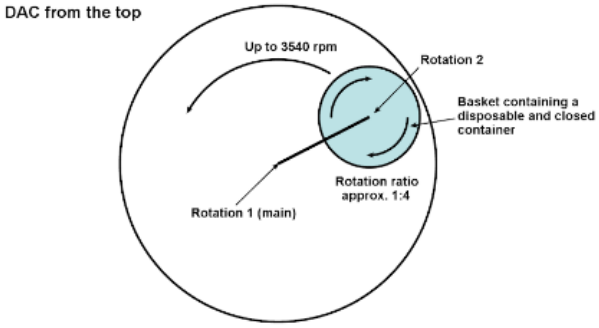

Figure 14: A schematic drawing of a dual asymmetric centrifuge [42]

In the literature, a DAC is used for the dispersion of carbon nanotubes in PDMS and carbon black/graphite nanoplatelets in epoxy [43][44].

2. Materials

A conductive blend is obtained by mixing a polymer with conductive fillers. Multiple combinations are reported in the literature because each conductive filler and polymer has unique characteristics and by judicious blending both materials, a spectrum of unique composites can be achieved. In the following paragraphs, the used polymer, fillers and machines will be discussed.

2.1 The polymer matrix: PDMS

Polydimethylsiloxane or PDMS is the used silicone elastomer in this thesis and it is the most commonly used silicone in literature. Besides silicones, acrylics and polyurethanes are also used for the fabrication of conductive composites. PDMS has exceptional properties such as chemical inertness, thermal stability, transparency, and viscoelasticity [3]. It is obtained by a polymerization reaction between dimethyldichlorosilane and water and it consists of a Si-O backbone with repeating units of Si(CH3)2O. The latter determines the molecular weight, which generally varies between 10 000 and 60 000 g/mol and the viscoelastic characteristics of the polymer [52].

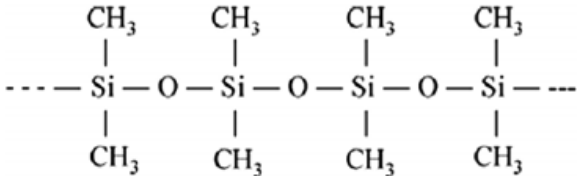

Figure 15: The chemical structure of PDMS [53]

The PDMS in this thesis is the SYLGARDTM 184 silicone elastomer kit from Dow Corning and the base is a viscous liquid that becomes flexible and rigid when the curing agent is added. The mixing ratio between base and curing agent is 10:1.

2.2 Conductive fillers

A conductive filler enhances the blend in a unique way, especially the viscosity and conductivity. The fillers discussed in this thesis include multi-walled carbon nanotubes, single-walled carbon nanotubes, both in powder form and suspension, carbon black, a mixture of carbon black and carbon nanotubes, silver coated copper flakes and a suspension of IPA and silver nanowires.

2.2.1 Single- and multi-walled carbon nanotubes

Carbon nanotube structures gain interest due to their intrinsic structural strength, which is appraised as one of strongest in nature. They are also corrosion resistant, very light and exhibit high thermal and electrical conductivity in the magnitude of 3000 W/(m·K) and 107 S/m, respectively. CNTs can be semiconducting or metallic, depending on the geometry [54]. The sp2 hybridization of carbon atoms in the seamless rolled up graphene sheets is the origin of these extraordinary characteristics. The most common nanotubes are the single-walled and multi-walled carbon nanotubes, exhibiting a high aspect ratio and a distinct atomic structure. Single-walled carbon nanotubes are cylinders of graphene, while multi-walled carbon nanotubes consist of multiple concentric SWCNTs.

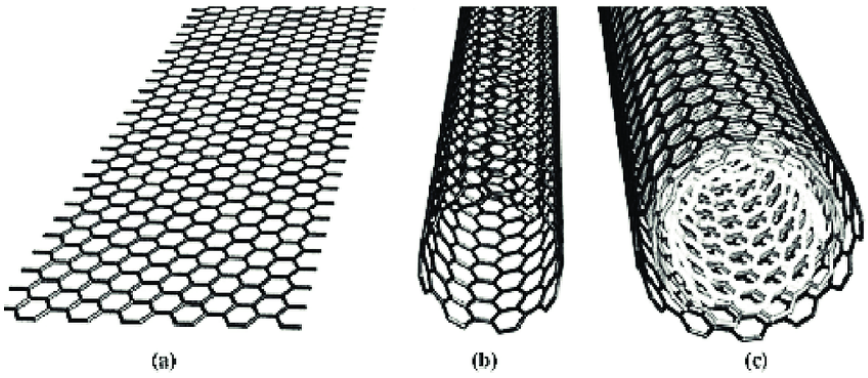

Figure 16: (a) a sheet of graphene, (b) a SWCNT and (c) a MWCNT [55]

There exist multiple synthesis methods for carbon nanotubes, including laser ablation, chemical vapor deposition and arc discharge [56]. Chemical vapor deposition yields the highest amount of CNTs because they are grown directly on a substrate, while CNT's are collected in laser ablation and arc discharge.

Thanks to their exceptional characteristics, CNTs are widely used as a conductive filler in conductive composites. The following table gives an overview of the achieved percolation thresholds of carbon nanotubes in the literature [27],[31],[33],[57],[59].

Table 1: The reported percolation thresholds of MWCNTs in the literature

Volume percentage of MWCNTs (vol%)	Weight percentage of the MWCNTs (wt%)	Fabrication method	Polymer matrix	Reference
0.13	0.28	Solution mixing	Polydimethylsiloxane (PDMS)	[27]
Incalculable (MWCNTS not specified)	5	Solution mixing	Polydimethylsiloxane (PDMS)	[31]
0.26	0.4	Shear mixing (exact method not specified)	Polydimethylsiloxane (PDMS)	[33]
0.06	0.1	Solution mixing	Polydimethylsiloxane (PDMS)	[33]
0.19	0.3	Solution mixing + shear mixing (exact method not specified)	Polydimethylsiloxane (PDMS)	[33]
Incalculable (unknown MWCNT density)	<1	Solution mixing	Polydimethylsiloxane (PDMS)	[57]

Table 2: The reported percolation thresholds of SWCNTs in the literature

volume percentage of the SWCNTs (vol%)	Weight percentage of the SWCNTs (wt%)	Fabrication method	Polymer matrix	Reference
0.33	0.33	Solution mixing	PMMA	[59]

While the magnitude of the percolation thresholds is similar, the difference in the aspect ratio of the used carbon nanotubes, and the fabrication method to a lesser extent, explain the deviations because an increased aspect ratio decreases the percolation threshold [18].

The examined multi-walled carbon nanotubes in this thesis are from Sigma-Aldrich, product no: 659258. The properties of the multi-walled carbon nanotubes are summarized in the following table [60].

Table 3: Main properties of the used multi-walled carbon nanotubes

Main properties MWCNTs	Value
Density	1.7 g/ml
Diameter	110 – 170 nm
Length	5 – 9 μm

Two types of single-walled nanotubes are used in this thesis, both are from OCSiAl. The first type are pristine SWCNTs in powder form and the second type is a suspension of PDMS oil and SWCNTs, named Matrix. Matrix consists of 90% PDMS oil and 10% SWCNT by weight. PDMS oil only affects the softness of the composite and can be treated as normal PDMS when calculating the weight percentages.

Table 4: Main properties of pristine single-walled carbon nanotubes [61]

Main properties SWCNTs	Value
Density	Not specified
Diameter	1.56 – 1.64 nm
Length	>5 μm

Table 5: Main properties of Matrix [62]

Main properties Matrix	Value
PDMS oil content	90 wt%
SWCNT content	10 wt%
Density	1.04 g/ml
Diameter (SWCNT)	1.56 – 1.64 nm
Length (SWCNT)	>5 μm

2.2.2 Carbon black

Carbon black is a collective name for all colloidal forms of carbon. It is a family of predominantly amorphous carbon particles which are agglomerated in various shapes and sizes. Carbon black has a general volume resistivity between 10-1 and 102 **Ω**.cm, making them suitable for enhancing the electrical properties of a composite. Besides conductive composites, carbon black is used for structural reinforcement and black pigments in ink or paint [63].

Carbon black is obtained by an incomplete combustion of carbonaceous materials and the synthesis process consists of the following steps;

1. Introducing carbonaceous materials in the combustion chamber
2. Partial or complete oxidation
3. Quenching the product with water

The process parameters such as temperature and reaction time affect the characteristics of the carbon black material. A higher temperature and shorter reaction time achieve smaller and highly structured particles [64].

Since it is a commonly used filler for conductive composites, the literature reports multiple percolation threshold as guidance. The following table gives an overview of the percolation thresholds, the fabrication method and the polymer matrix [3],[65].

Table 6: Multiple reported percolation thresholds of CB

Volume percentage of CB (vol%)	Weight percentage of CB (wt%)	Fabrication method	Polymer matrix	Reference
61.16	43.03	Manual mixing	Polydimethylsiloxane (PDMS)	[3]
42.36	16.66	High speed mixing	Polydimethylsiloxane (PDMS)	[65]

The examined carbon black in this work is the micron super adsorption activated porous carbon powder from US Research Nanomaterials, product no: US 1143M. The most important properties of the material are outlined in the following table [66].

Table 7: Main properties of the used carbon black material

Main properties CB	Value
Average diameter	10 µm
Density	0.47 g/ml
Intrinsic electrical resistivity	0.32 Ohm.cm

2.2.3 Mixture of carbon black and carbon nanotubes

While extensive research is done on pristine fillers such as carbon nanotubes and carbon black as conductive fillers for composites, sparse research is conducted on the possibilities of hybrid fillers. Zheng et al. investigated the mechanism of a hybrid filler consisting of carbon black and multi-walled carbon nanotubes. For the hybrid system, the gaps between adjacent nanotubes are filled with the carbon black particles and a conductive pathway is synergistically created through the polymer matrix [67].

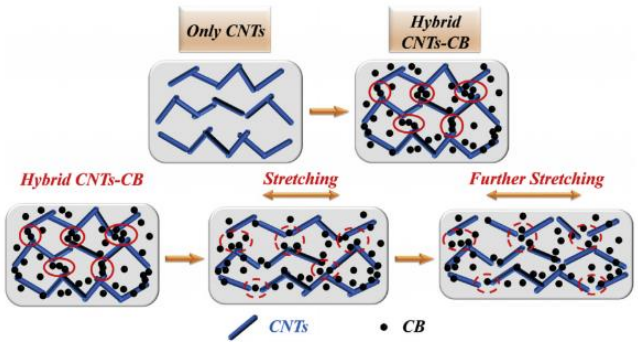

Figure 17: The conduction mechanism in hybrid fillers [67]

If the carbon nanotubes are separated from each other during stretching, the particles will rearrange and carbon black particles could relocate themselves in order to maintain the conductivity [67].

The following table gives an overview of the reported percolation thresholds for mixtures of carbon black and carbon nanotubes but the values are highly dependent of the mixing ratio, particle size and intrinsic conductivity of the particles [3],[68].

Table 8: Reported percolation thresholds of the mix of carbon nanotubes and carbon black

Volume percentage of hybrid filler (vol%)	Weight percentage of hybrid filler (wt%)	Fabrication method	Polymer matrix	reference
Incalculable (unknown polymer)	1-3	Not specified	Not specified	[68]
28.04	5.68	Manual mixing	Polydimethylsiloxane (PDMS)	[3]

Super conductive carbon black nanopowder and carbon nanotubes from US Research Nanomaterials, product no: US4899 is the examined mixture in this thesis. Although the mixing ratio is unknown, the characteristics of the material are shown in the following table [68].

Table 9: Main properties of the carbon black and carbon nanotube mixture

Main properties CNTs + CB	Value
Diameter CB	5 – 100 nm
Diameter CNTs	30 – 100 nm
Length CNTs	5 – 30 µm
Density	0.15 g/ml
Intrinsic electrical resistivity	2 – 5 x 10^{-4} Ohm.cm

2.2.4 Silver coated copper flakes

Silver coated copper flakes are a good alternative for pristine silver particles due to their quality, electrical conductivity and cost-price ratio. However, copper can migrate through the silver coating where it can oxidize and thus increase the resistivity of the particles. Furthermore, the migration rate increases as the temperature increases [69].

The synthesis method for the flakes consists of coating a copper nucleus with silver and in order to do this, a chelating agent is used. A chelating agent is a compound which binds molecules and ions to metal ions. First, a slurry is made with the copper powder and chelating agent. Next, a silver ion solution is added to the suspension and mixed thoroughly. Afterwards, a reducing agent is added in order to form a silver coat on the copper nuclei and the resulting powder is filtrated and washed [70].

While it is an uncommon filler for stretchable conductive composites, the following table shows the reported percolation thresholds in the literature [3],[71]

Table 10: Reported percolation thresholds of Ag coated Cu flakes.

Volume percentage of Ag coated Cu flakes (vol%)	Weight percentage of Ag coated Cu flakes (wt%)	Fabrication method	Polymer matrix	reference
Incalculable (unknown filler density)	75	Not specified	Polydimethylsiloxane (PDMS)	[71]
15.18	63	Manual mixing with a small amount of THF	Polydimethylsiloxane (PDMS)	[3]

EConduct Copper 042500 from Eckart, product no: 010359B10 is the used material in this work and the main properties are summarized in the following table [72].

Table 11: Main properties of the used Ag coated Cu flakes

Main properties Ag coated Cu flakes	Value
Average diameter	D90 - 9 μm
Density	Not specified (9.34 g/ml according to similar products)
Amount of copper	75 - 72 wt%
Amount of silver	25 - 28 wt%

2.2.5 Silver nanowires

Silver nanowires are one of the most promising nanofillers for the fabrication of stretchable electronics since nanowires exhibit the highest aspect ratio of all nanomaterials and silver has the highest thermal and electrical conductivity of all metals [73].

The most common method for synthesizing silver nanowires is the polyol method. The materials of the reaction includes AgNO3 as the silver precursor, ethylene glycol (EG) as reducing agent and solvent and finally polyvinylpyrrolidone (PVP) as a capping agent. The reaction involves heating EG to a specific temperature and adding PVP and AgNO3. The reaction time, temperature and AgNO3:PVP ratio are important parameters in order to control the growth process of silver nanowires [73].

Silver nanowires are widely used for creating stretchable and transparent electrodes and the fabrication process consists of embedding the silver nanowires in the surface [74-77]. Bulk dispersion of silver nanowires is sparsely researched but the following table shows the reported percolation thresholds [78-80].

Table 12: Percolation thresholds of bulk dispersed silver nanowires

Volume percentage of Ag nanowires (vol%)	Weight percentage of Ag nanowires (wt%)	Fabrication method	Polymer matrix	reference
Incalculable (unknown filler density)	9.09	Solution mixing	Polyvinyl alcohol (PVA)	[78]
1.8	16.40	Solution mixing	Polyvinylidene fluoride (PVDF)	[79]
0.6	Incalculable (unknown filler density)	Solution mixing + mold casting	Poly(vinylidene fluoride–trifluoroethylene) - P(VDF-TrFE)	[80]
2.2	Incalculable (unknown filler density)	Solution mixing + mold casting	Poly(vinylidene fluoride–trifluoroethylene) - P(VDF-TrFE)	[80]

Silver nanowires in an isopropyl alcohol suspension (0.5 wt% silver nanowires) from Sigma-Aldrich, product no: 739421 are the used nanowires in this thesis. The properties of the material are summarized in the following table [81].

Table 14: Main properties of the used silver nanowires

Main properties silver nanowires	Value
Density	10.49 g/ml
Diameter	50 – 70 nm
Length	5 – 15 μm

2.3 The used machines in this work

For the manual mixing experiments, a plain spatula and glass plate were used. For solution mixing, a magnetic stirrer was used in order to mix multiple samples simultaneously. The ball milling, speed mixing and roll milling experiments used more specialized machines and are listed in the following table.

Table 15: Used machines in this thesis

Machine	Model
Ball mill	Planetary Micro Mill PULVERISETTE 7, premium line from Fritsch
Three roll mill	T50 Ointment Mill from Torrey Hills Technologies
High speed mixer	High speed mixer: DAC 150.1 FVZ-K from FlackTek Inc.

3. Measurements and results

3.1 Conductivity of bulk powders

Oxidation, impurities, etc. have a negative influence on the conductivity of the materials. In order to ensure the conductivity of the used powders, a set-up was built according to the methodology of the following figure.

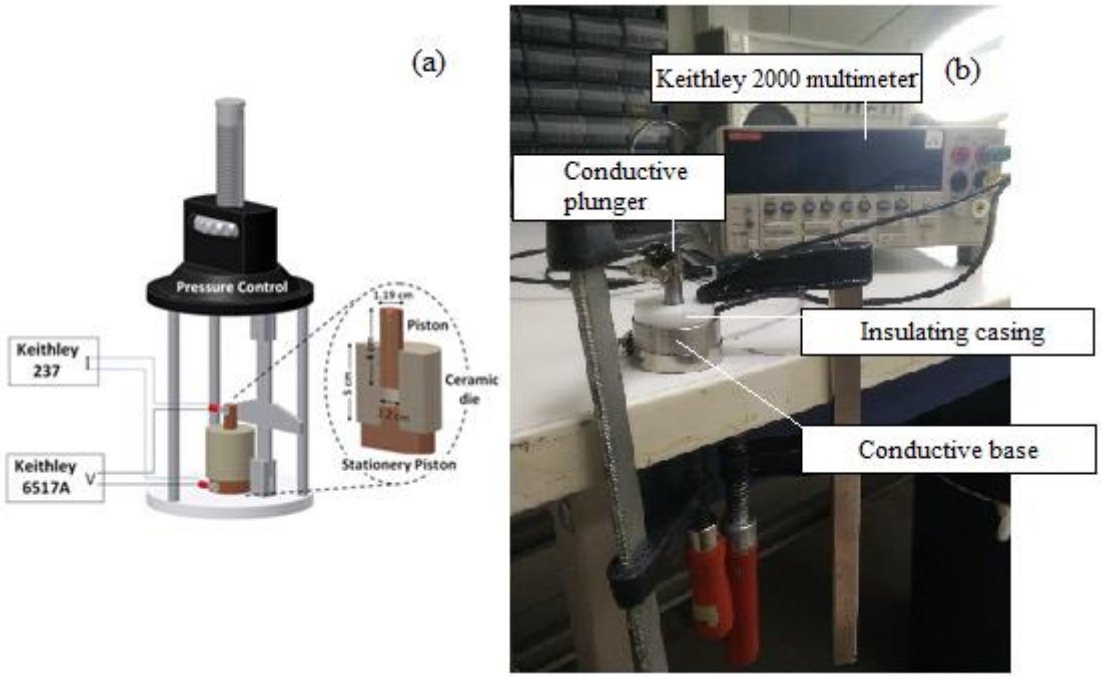

Figure 18: Conceptual schematic of a powder press (a) and experimental implementation (b) [82]

An cylindrical insulating material acts as the casing of the compression chamber. A conductive base closes the bottom of the chamber while a tight-fitting conductive plunger seals the chamber. The conductive parts act as the electrodes for performing a two-wire resistance measurement. When a precise amount of powder is added into the chamber, a load is applied to the plunger in order to compress the powder to ensure optimal contact between the particles. The applied pressure increases the conductivity of the powder due to the removal of air bubbles and the increased contact area [82]. Once the powder is thoroughly compressed, the bulk resistivity can be calculated with the following formula [83]:

$$\rho = \frac{R * A}{h}$$

Formula 1: The resistivity of bulk powders [83]

With ϱ the resistivity of the powder in **Ω***m, R the resistance in **Ω**, A the surface of the compressed powder disk in m2 and h the height of the disk in m.

The implemented powder press consists of inox and the inner diameter of the compression chamber is 8 mm. A two-wire resistance measurement is performed with a Keithley 2000 multimeter. The whole set-up is fastened with a clamp, while an additional clamp is used to press the plunger into the compression chamber.

The following progressive scheme is used in order to measure the resistivity of the bulk powders:

1. As a reference point, an empty chamber is compressed and the initial height between the bottom of the clamp and the top of the insulating base is measured with a digital caliper while the initial resistance of the set-up is measured with the Keithley multimeter.

2. The compression chamber is filled with powder and the powder is repeatedly compressed with the plunger until a smooth layer is achieved.

3. The powder is compressed one more time and the final resistance and height are measured.

When calculating the resistivity of the powder, it is important to use the difference between the initial values of the height and weight and the final values of the height and weight in order to avoid miscalculations. The difference between the initial and final height is the height of the compressed disk while the difference between the final and initial resistance is the resistance of the disk. The following table shows the calculated resistivity of the used powders in comparison with the values provided by the manufacturer [61],[66],[68],[72],[81]. MWCNTs and Matrix could not be tested since there was a shortage of MWCNTs and the PDMS oil in Matrix inhibited accurate measurements.

Table 16: Resistivity of bulk powders

Material	Measured resistance of disk (**Ω**)	Height of disk (m)	Calculated resistivity	Resistivity provided by the manufacturer
Carbon black	0.070	1.8×10^{-4}	1.95×10^{-2} **Ω***m	3.2×10^{-3} **Ω***m
Carbon black & CNTs	0.002	1.5×10^{-4}	6.70×10^{-4} **Ω***m	$2 - 5 \times 10^{-6}$ **Ω***m
Silver coated copper flakes	0.001	1.5×10^{-4}	3.35×10^{-4} **Ω***m	Not specified
Pristine SWCNTs	0.001	1.0×10^{-4}	5.02×10^{-4} **Ω***m	Not specified
Silver nanowires	0.011	1.2×10^{-4}	4.61×10^{-3} **Ω***m	Not specified

The silver nanowires required a different approach because they were dissolved in IPA. Therefore, the suspension was added in small amounts under air extraction equipment in order to evaporate the solvent. A thin layer of silver nanowires coated the inside of the compression room and the resistance was measured. Against the expectations, the silver nanowires exhibited one of the highest resistances. A possible cause could be the presence of a very small amount of IPA in the compressed disk, resulting in an increased resistance.

The differences between the calculated and actual values can be explained due to accuracy of the measurement set-up. Suboptimal compression and contact between the connectors and the powder press cause measurement errors. However, the measurements give an indication of the resistivity of the used powder and ensure their conductivity.

3.2 Comparison of dispersion techniques

A good dispersion state of the fillers within the polymer matrix is required to ensure the elastic properties of the composite. Therefore, a comparative study is conducted between multiple dispersion techniques in order to determine the best one. Solution mixing (SM), ball milling (BM), three roll milling (TRM) and high speed mixing (HSM) are the techniques of choice. To ensure comparable results, each sample contains the same amount of materials.

Table 17: The used materials for each sample

Carbon black (g)	Component A of PDMS (g)	Component b of PDMS (g)
0.63	6.00	0.66

The comparison of the samples is based on SEM images which are taken under the same circumstances and at the same locations within the samples. The following section describes the utilised progressive schemes for each dispersion method.

3.2.1 Solution mixing

For solution mixing, the method of Zheng et al. was used to disperse carbon black within PDMS [27]. The following steps were performed:

1. Carbon black is dissolved in 15 ml xylene and the suspension is sonicated in an ultrasonic bath for 20 minutes.

2. Component A of PDMS is dissolved in xylene with a volume ratio of 1:1.

3. Both suspensions are simultaneously stirred with a magnetic stirrer at 1400 RPM for 1 hour.

4. The two suspensions are mixed and the resulting suspension is stirred at 2000 RPM for 1 additional hour.

5. The curing agent is added and the final suspension is mixed at 2000 RPM for 30 minutes.

6. The suspension is placed in low vacuum for 10 minutes in order to remove any air bubbles.

7. After the vacuum, the suspension is placed under a fume hood for 24 hours to evaporate the remaining solvent.

8. Finally, the sample is obtained by curing the suspension in a standard oven at 100°C for 20 minutes.

During the solution mixing process, it is important to not stir the suspension if there are two separate layers after the 24 hour evaporation. During the initial testing, xylene was separated from the PDMS mixture. The mixture was stirred to obtain a homogenous blend but it did not cure because of the presence of xylene. To solve this problem, the sample can be placed in low vacuum for a second time to accelerate the evaporation of xylene.

3.2.2 Ball milling

For ball milling, the progressive scheme wasn't based on a published paper but on the recommendations of fellow researchers:

1. Carbon black and component A of PDMS are mixed twice at 250 RPM for 3 minutes and twice at 250 RPM for 6 minutes, resulting in a total mixing time of 18 minutes. Halfway through each mixing period, the walls of the container are cleaned.

2. The curing agent is added and the suspension is mixed twice at 250 RPM for 6 minutes and the walls are cleaned every 3 minutes.

3. The suspension is placed in low vacuum for 10 minutes to remove the present air bubbles.

4. The suspension is cured at 100 °C for 20 minutes in a standard oven.

3.2.3 Three roll milling

Similar to ball milling, the progressive scheme for three roll milling is based on the recommendations of a fellow researcher:

1. Carbon black and component A of PDMS are mixed. Subsequently, a cycle through the three roll mill is executed with the following settings:

Table 18: Initial settings of the three roll mill (T50 Ointment Mill from Torrey Hills Technologies)

Speed setting	Front gap size	Rear gap size
2	30 µm	46 µm

2. Afterwards, the rear gap size setting is reduced to 28 µm and 4 more cycles are executed.

3. The curing agent is added and the suspension is mixed by hand

4. The suspension is placed in low vacuum for 10 minutes to remove air bubbles.

5. The sample is obtained by curing the suspension at 100°C for 20 minutes.

3.2.4 High speed mixing

The following steps describe the high speed mixing process, which are based on the work of Ganguli et al. and experimental trials [84].

1. Component A of PDMS and carbon black are mixed at 3400 RPM for 8 minutes. At 4 minutes, the walls of the container are cleaned and the mixing is resumed.

2. The curing agent is added and the resulting suspension is mixed at 3400 RPM for 2 minutes whereby the walls are cleaned halfway through.

3. The suspension is placed in vacuum for 10 minutes in order to remove air bubbles.

4. The sample is obtained after curing the suspension at 100°C for 20 minutes.

It is important to choose the right container for a sample since the container has to be filled halfway to guarantee proper mixing, as stated by the owner of the machine.

3.2.5 Comparison

In order to visualize the composites with SEM, small samples were cut out of the composite and a 8 nm layer of carbon was deposited. Afterwards, the samples are attached to the sample holder of the microscope with silver paste and low vacuum is applied. The following figure shows the SEM images of the samples which are fabricated with solution mixing, ball milling, three roll milling and high speed mixing.

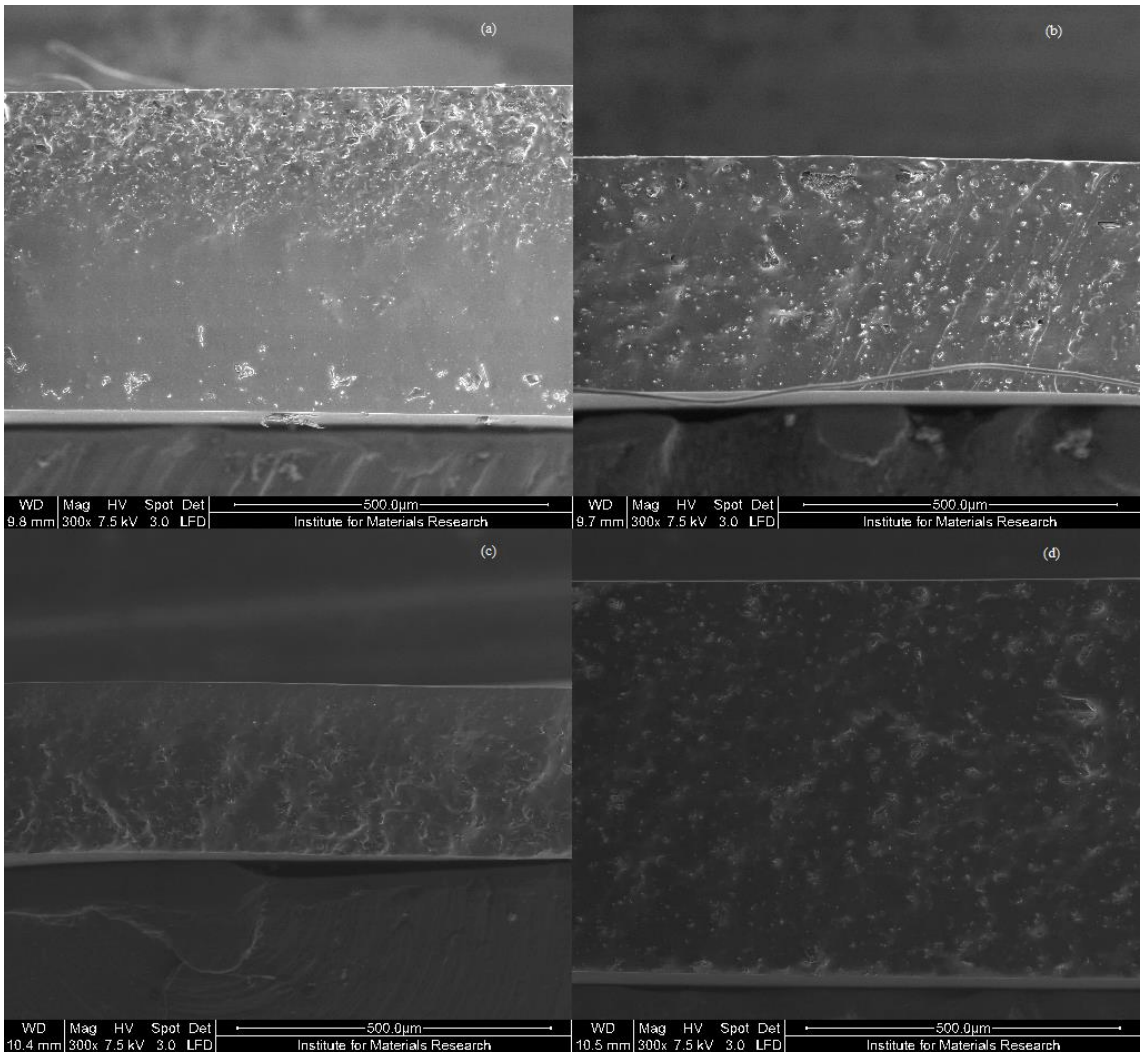

Figure 19: Comparison of the SEM images of each sample whereby (a) is fabricated by SM, (b) is fabricated by BM, (c) is fabricated by TRM and (d) is fabricated by HSM

With a 300 x magnification, remarkable differences can be seen in terms of homogeneity. While the samples produced by BM, TRM and HSM are homogenous, the sample produced by SM exhibits two phases within the sample.

This can be explained by the overnight evaporation of the solvent. Since the suspension has not cured yet, the carbon black particles can sink to the bottom of the Petri dish. When the sample is eventually cured, the composite hardens which results in a carbon black rich and carbon black poor area, as depicted in the above figure. Out of the four samples, three roll milling and high speed mixing yield the most homogenous samples.

Homogeneity is just one parameter to judge the dispersion state of the filler. The presence of the particle agglomerates is also important since agglomerates increase the required amount of conductive filler for percolation. This counteracts the benefit of using state of the art fillers which achieve percolation with low filler amounts. In order to compare the amount of the agglomerates, a closer look is taken at the agglomerate rich areas of figure 19.

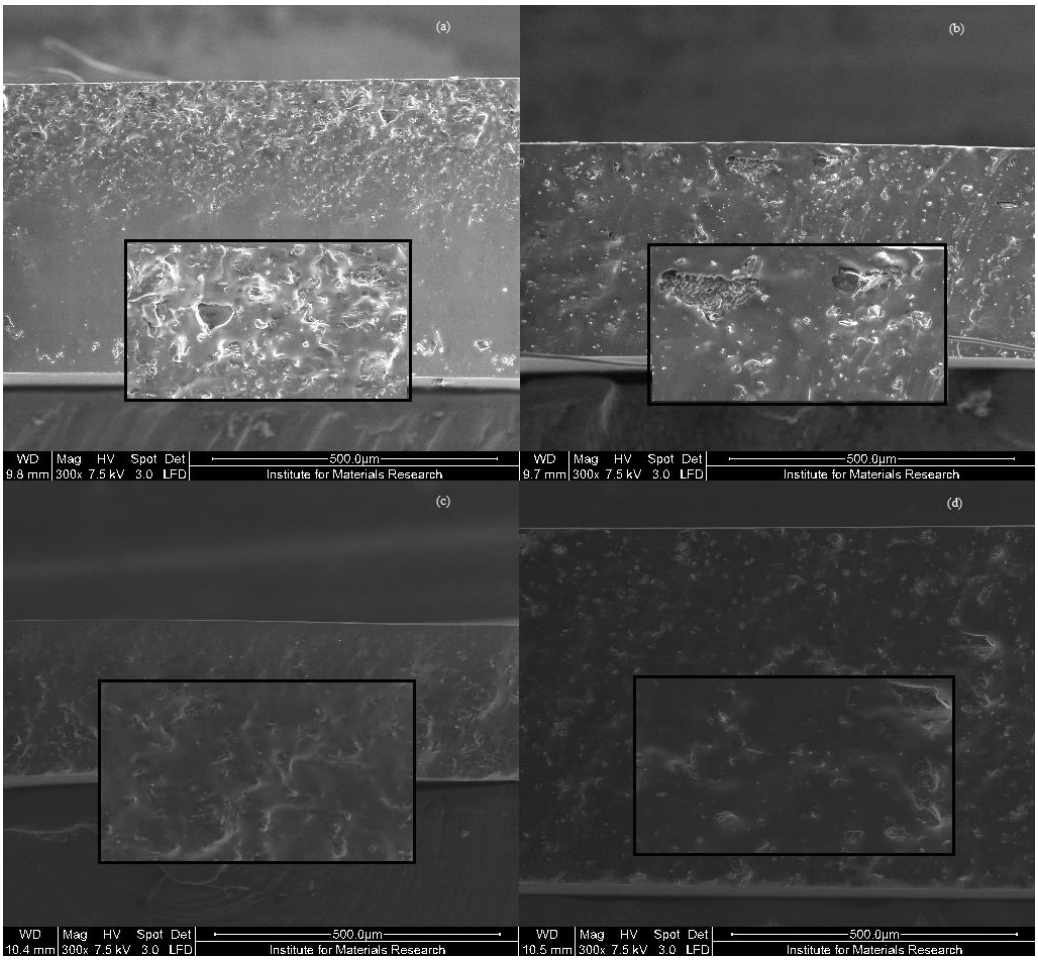

Figure 20: A closer look at the agglomerate rich areas of the samples fabricated by (a) SM, (b) BM, (c) TRH and (d) HSM. The scale of the zoomed in areas is different from the indicated scale at the bottom of the figure

The highest amount of agglomerates are produced by solution mixing. A possible explanation can be that during 24 hour evaporation of xylene, no external forces from techniques such as sonication or shear mixing are present to separate the filler

particles, so the attraction between the particles dominates, resulting in the formation of agglomerates [35]. However, the biggest agglomerates are produced by Ball milling, followed by solution mixing, high speed mixing and three roll milling.

Based on the amount of agglomerates and homogeneity of the composite, three roll milling and high speed mixing offer the highest dispersion quality, which will be the dispersion methods of choice for the percolation experiments.

3.3 Percolation experiments

During these experiments, the percolation threshold is determined of seven conductive particles, including a mixture of carbon black and carbon nanotubes (CB & CNTs), single-walled carbon nanotubes in PDMS oil (Matrix), pristine single-walled carbon nanotubes (SWCNTs), multi-walled carbon nanotubes (MWCNTs), carbon black (CB), silver coated copper flakes (Ag coated Cu flakes) and silver nanowires (Ag nanowires).

The chosen percolation thresholds for examination were based on the literature and refined after each step. For each step, a specific amount of material is weighed and dispersed by using either three roll milling or high speed mixing as described in the previous section. A blade coater was used in order to create uniform samples. In order to check if the percolation threshold is passed, the resistance of a square sample is measured by using a Fluke multimeter with a measurement limit of 50 M**Ω**. Composite resistances above 50 M**Ω** are considered non-conductive.

3.3.1 Mixture of carbon black and carbon nanotubes in PDMS

The dispersion method of choice is high speed mixing due to the efficiency and homogenous dispersion. During high speed mixing, samples were taken for quality control by smearing a small amount of suspension onto a clear surface to ensure no visible agglomerates were present. The initial weight percentages of CB & CNTs are 3 wt% until 15 wt%, with an increment of 3 wt% for each step. After the initial resistance measurements, the sample with a filler content of 6 wt% was the first conducting sample, meaning the percolation threshold was located between 3 wt% and 6 wt%. Additional samples with a filler content of 4 wt% and 5 wt% were made but none of them were conductive, resulting in a percolation threshold around 6 wt%.

Table 19: Resistance and logarithm of resistance per weight percentage of CB &CNTs

Volume percentage CB &CNTs (vol%)	Weight percentage CB &CNTs (wt%)	Resistance (Ω)	Logarithm of resistance (Ω)
0	0	No value	No value
16.67	3	No value	No value
21.23	4	No value	No value
25.39	5	No value	No value
29.22	6	75000	4.86
39.01	9	3200	3.51
46.86	12	1800	3.26
53.30	15	269	2.43

The 'no value' implies a measured resistance which is higher than 50 MΩ, the measurement limit of the Fluke multimeter. The logarithm of the resistance is taken in order to visualize the resistance drop in the following graph:

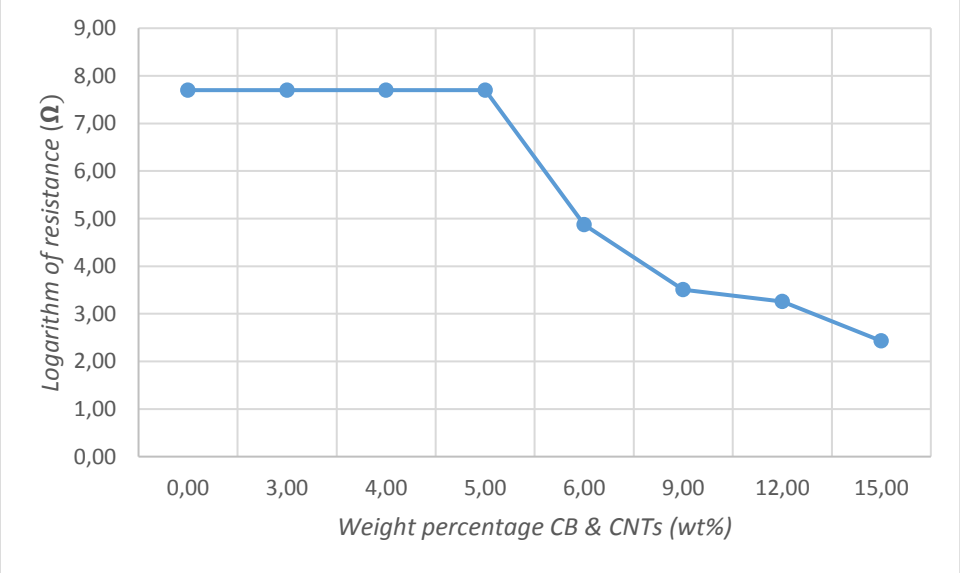

Figure 21: Logarithm of resistance as a function of weight percentage CB and CNTs

The resulting percolation threshold of 6 wt% (29.22 vol%) is comparable to the reported values in the literature. However, the percolation threshold is slightly lower than the reported percolation thresholds of pristine carbon black, indicating that the addition of high aspect ratio fillers lowers the percolation threshold of low aspect ratio fillers [86]. Finally, the typical resistance drop around the percolation threshold is clearly visible and as the wt% increases further, the increase in conductivity starts to stagnate.

3.3.2 Multi-walled carbon nanotubes in PDMS

High speed mixing is the dispersion method of choice for the MWCNTs. Unfortunately, due to a shortage of MWCNTs, only two weight percentages are tested, based on the previous work [3]. The weight percentages of choice are 9 wt% and 12 wt%. The resistance and logarithm of resistance for each wt% is listed in the following table.

Table 20: Resistance and logarithm of resistance per weight percentage of MWCNTs

Volume percentage MWCNTs (vol%)	Weight percentage MWCNTs (wt%)	Resistance (Ω)	Logarithm of resistance (Ω)
0	0	No value	No value
5.34	9	1.32×10^6	6,120574
7.22	12	23000	4,361728

Due to the shortage of material, only two samples were made thus it is impossible to accurately pinpoint the percolation threshold of MWCNTs. Nonetheless, the sharp decrease in resistance between 9 wt% (5.34 vol%) and 12 wt% (7.22 vol%) indicates the percolation threshold is located around 9 wt%, which corresponds to the percolation threshold of 9.03 wt% of the previous work [3].

3.3.3 Single-walled carbon nanotubes in PDMS oil (Matrix) in PDMS

High speed mixing is used to disperse the initial single-walled carbon nanotubes (Matrix). During the weighing process of the material, it is important to take into account that Matrix only contains 10% SWCNT by weight. For example, if a sample requires a SWCNT content of 3 wt%, the composite consists of 30 wt% Matrix and 70 wt% PDMS. During the fabrication process of the composite, samples for quality control are taken. The initial percolation thresholds for examination were 1 wt%, 3 wt%, 5 wt%, 7 wt% and 9 wt% SWCNT. All of the samples were conductive, meaning the percolation threshold is located below 1 wt% SWCNT. The following range of weight percentages, namely 0.2 wt% until 0.8 wt% with an increment of 0.2 wt% per step were created with high speed mixing, but agglomerates were present. This can be explained due to suboptimal mixing since the container wasn't filled halfway and a smaller container was required. However, there was no smaller size available at the time so it opted to use the three roll mill instead. The chosen percolation thresholds were 0.05 wt%, 0.10 wt%, 0.15 wt%, 0.25 wt% and 0.35 wt%.

The recommend processing guidelines of the manufacturer were utilised, namely performing 20 three roll mill cycles in total. The following steps were performed:

1. A suspension of component A and the filler with a known ratio is added to the three roll mill.

2. Ten cycles are performed with the following settings:

Table 21: Settings of the three roll mill (T50 Ointment Mill from Torrey Hills Technologies)

Speed setting	Front gap size	Rear gap size
2	30 µm	28 µm

3. The suspension is recuperated as much as possible and added in a small container with a known weight. The amount of suspension is weighed and the required component B is calculated and added.

4. The suspension is initially mixed by hand before an additional 10 mill cycles are performed with the same settings.

5. The suspension is placed in vacuum for 10 minutes to remove the present air bubbles.

6. The suspension is cured at 100 °C for 20 minutes in a standard oven.

The following table lists the corresponding resistance and logarithm of resistance for each weight percentage of single-walled carbon nanotubes in Matrix. The distinct drop in resistance around the percolation threshold is also illustrated.

Table 22: Resistance and logarithm of resistance per weight percentage of SWCNTs (in Matrix)

Volume percentage SWCNTs (vol%)	Weight percentage SWCNTs (wt%)	Resistance (**Ω**)	Logarithm of resistance (**Ω**)
Incalculable (unknown pristine SWCNT density)	0	No value	No value
Incalculable	0.05	No value	No value
Incalculable	0.10	2.24×10^{7}	7.35
Incalculable	0.15	6.95×10^{6}	6.84
Incalculable	0.25	2.30×10^{6}	6.36
Incalculable	0.35	1.20×10^{6}	6.08

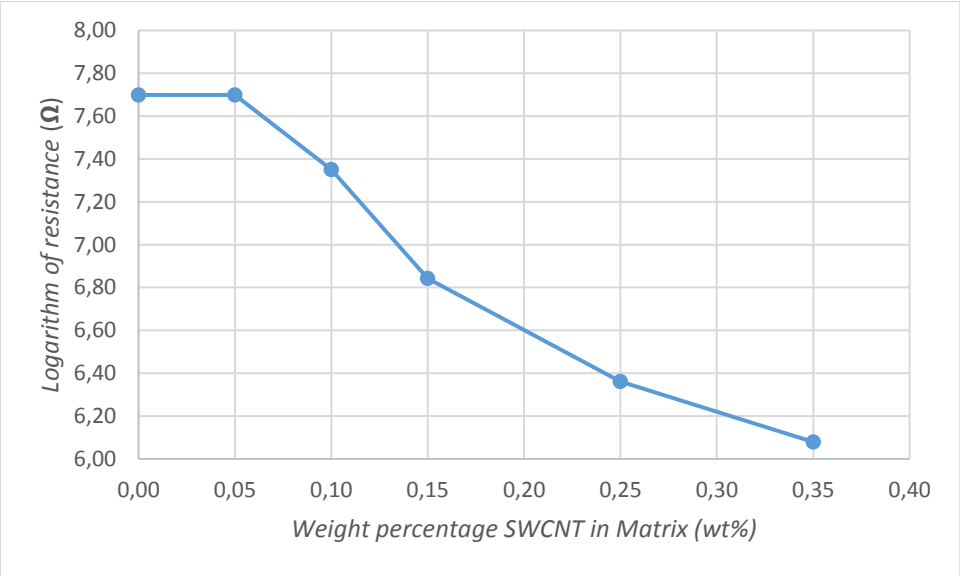

Figure 22: Logarithm of resistance as a function of weight percentage of SWCNTs (in Matrix)

The percolation threshold of SWCNTs is situated around 0.10 wt% which is in the same magnitude of the reported thresholds in the literature. The low percolation threshold can be explained by the high aspect ratio of the carbon nanotubes, which greatly reduces the percolation threshold [18]. However, at these low weight percentages of SWCNTs, the composites are not usable for stretchable electronics due to the high resistance, which is in the magnitude of M**Ω**s.

3.3.4 Pristine single-walled carbon nanotubes in PDMS

Since the pristine SWCNTs are the actual SWCNTs of Matrix, it was opted to test the same narrow range of weight percentages and to use the same dispersion method, namely three roll milling. The following table lists the results of the percolation experiment and the percolation phenomenon is illustrated.

Table 23: Resistance and logarithm of resistance per weight percentage of pristine SWCNTs

Volume percentage SWCNTs (vol%)	Weight percentage SWCNTs (wt%)	Resistance (**Ω**)	Logarithm of resistance (**Ω**)
Incalculable (unknown pristine SWCNT density)	0	No value	No value
Incalculable	0.05	No value	No value
Incalculable	0.10	2.23×10^7	7.37
Incalculable	0.15	1.55×10^7	7,190892

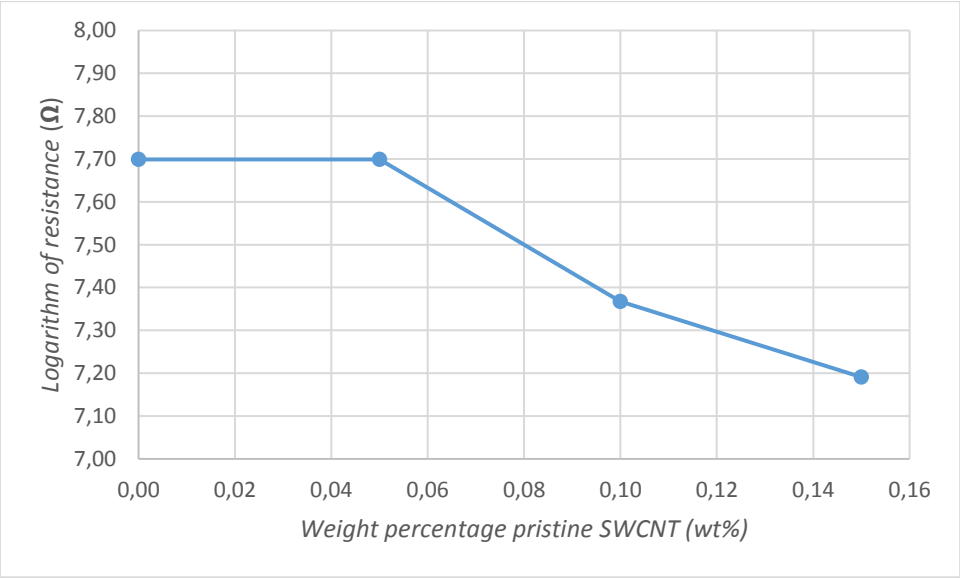

Figure 23: Logarithm of resistance as a function of weight percentage of pristine SWCNTs

As expected, the percolation threshold is located around the same weight percentage of SWCNTs in Matrix, namely 0.10 wt%. The difference in resistance at 0.15 wt% between the pristine SWCNTs and Matrix can be explained due to the suboptimal contact area of the sample and probes of the multimeter since the probes are manually pressed against the sample.

3.3.5 Carbon black in PDMS

Carbon black was dispersed by using the high speed mixer. The chosen percolation thresholds are based on the previous work, namely 32 wt%, 36 wt%, 40 wt% and 44 wt%. Unfortunately, the percolation threshold wasn't reached. Only the samples with carbon black content of 32 wt% and 36 wt% could be cured and these were not conductive. A possible explanation for why the last two samples could not be cured is the presence of sulphur. The datasheet of the used PDMS, Sylgard 184 from Dow Corning, indicates that the presence of sulfur could inhibit the curing process. Since carbon black is produced by the combustion of carbonaceous materials, sulfur dioxide is a source for sulfur and small amounts are present in carbon black [87]. When the samples contain 40 wt% and 44 wt% carbon black, the sulfur content can be too high, thus hindering the curing process.

3.3.6 Silver coated copper flakes in PDMS

A high speed mixer was used to disperse the Ag coated Cu flakes in PDMS. Samples with weight percentages of 57 wt%, 60 wt%, 63 wt%, 66 wt% and 69 wt% Ag coated Cu flakes were made but none of them were conductive. Higher amounts were technically possible but the cured sample of 69 wt% silver coated copper flakes was already too soft to be useful for stretchable applications, so the percolation

experiments were stopped. A possible solution could be the reduction of the blend viscosity by adding a solvent, as performed by the previous work [3].

3.3.7 Silver nanowires in PDMS

The dispersion method of choice for the silver nanowires in PDMS was the three roll mill. The initial weight percentages of the nanowires were 0.05 wt%, 0.10 wt% and 0.15 wt%. While the samples had a homogenous dispersion, they were not conductive. The additional sample with the remaining nanowires contained a lot of IPA and in order to accelerate the evaporation, the sample was placed in a vacuum oven at a low heat of 40 °C as advised by a fellow researcher. However, the reduced boiling point of IPA due to the applied vacuum caused the sample to boil and the sample spilled in the oven, resulting in a sample with an unknown ratio of PDMS and filler. The percolation experiment had to be stopped due to a shortage of nanowires.

3.3.8 Comparison of the different fillers

In this paragraph, a comparison between the found percolation thresholds of the fillers is made. The percolation thresholds of carbon black, silver coated copper flakes and silver nanowires were not reached and thus these fillers will not be discussed. The following table lists the found thresholds.

Table 24: Comparison of the found percolation thresholds of the fillers

Filler	Volume percentage (vol%)	Weight percentage (wt%)	Resistance (**Ω**)
CB & CNTs	29.22	6	7.50×10^4
MWCNTs	5.34	9	1.32×10^6
SWCNTs in PDMS oil (Matrix)	Incalculable (unknown pristine SWCNT density)	0.10	2.24×10^7
Pristine SWCNTs	Incalculable (unknown pristine SWCNT density)	0.10	2.23×10^7

When comparing the volume percentages of the filler at each percolation threshold, a pattern is observed. The mixture of carbon black and CNTs, which consists of 75% spherical carbon black, has a noticeably higher percolation threshold than the cylindrical single- and multi-walled carbon nanotubes. This indicates that the percolation threshold is lowered when the aspect ratio of the filler is increased. This claim is further confirmed when the aspect ratios of the carbon nanotubes is compared.

Table 25: Comparison of the aspect ratio of carbon nanotubes

Filler	Average length (μm)	Average diameter (nm)	Aspect ratio
MWCNTs	7	140	50
SWCNTs	5	1.60	3125

The percolation threshold of multi-walled carbon nanotubes is two orders of magnitude higher than the threshold of single-walled carbon nanotubes, while the aspect ratio is two orders of magnitude smaller than the aspect ratio of single-walled carbon nanotubes. This observation is in agreement with the literature [18].

3.4 Characterisation of the composites

The relationship between the relative resistance (ΔR/R0) and relative elongation (ΔL/L0) , namely the gauge factor (GF), is determined of each specimen. The gauge factor is an interesting characteristic of the composite because if the relative resistance remains unchanged during stretching, no conductivity is lost. This behaviour is favorable for stretchable electronic circuits since a constant resistance is required during deformations. When the specimen has a high gauge factor, it exhibits a good sensitivity for deformations, making it an ideal candidate for strain sensor applications.

In order to determine the gauge factor, the samples are elongated while the resistance is measured simultaneously. Each conducting sample was cut out of the cured composite by utilising a laser cutter (Trotec Speedy 100). The shape was rectangular with a length of 5 cm and width of 1 cm and a thickness of 1 mm.

The measurement set-up consists of a LabVIEW-controlled stretching apparatus and a Keithley 2000 multimeter which performs a four-wire resistance measurement. The top of the clamped sample is in contact with Kapton tape, which is an insulator, while the bottom is in contact copper tape. The multimeter is connected with the copper tape and the collected data from both the multimeter and stretching apparatus is processed in LabVIEW. The following figure shows the whole set-up.

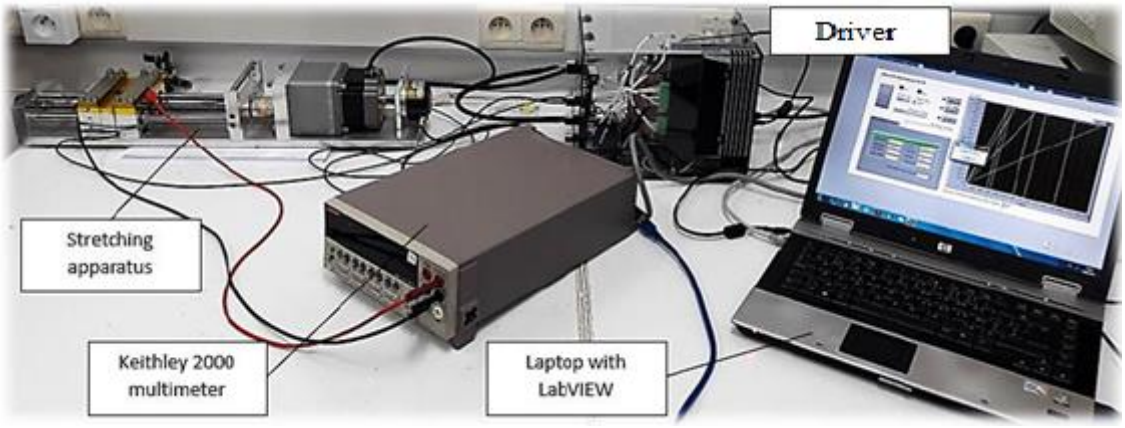

Figure 24: The complete measurement set-up [3]

3.4.1 Composite of Carbon black & carbon nanotubes and PDMS

The samples which passed the percolation threshold are tested on extensibility and the change in resistance. The four samples are expressed by the relative resistance as a function of relative elongation. The gauge factor is the slope of the graph in a certain point and the results are shown in the following figure.

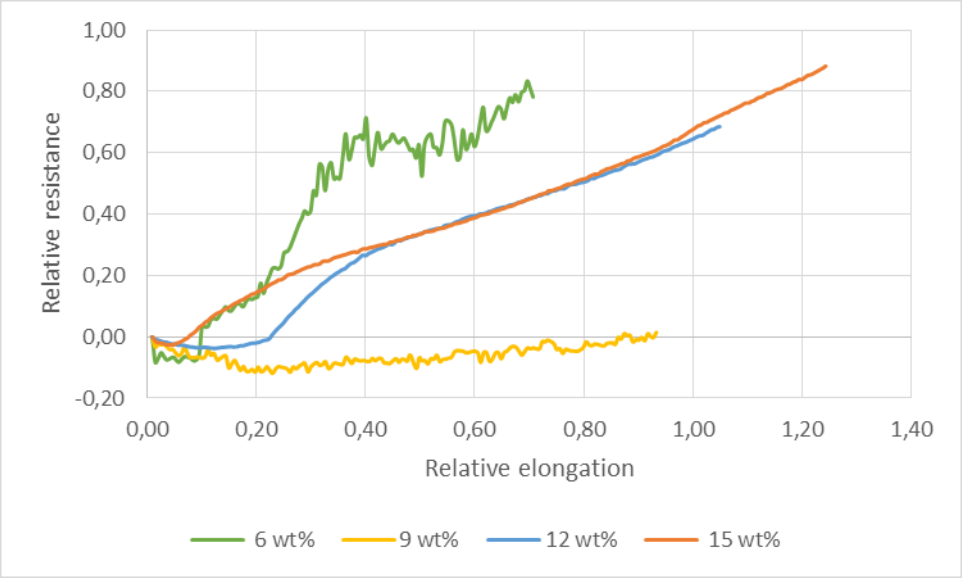

Figure 25: The relative resistance as a function of relative elongation of PDMS/ CB & CNTs composites

The resistance of each specimen is reduced during the initial relative elongation of 10% but the resistance increases with further stretching. The drop of resistance is explained by the repositioning of the CNTs since additional entanglement occurs during stretching. When the stretching increases, the entanglements are torn apart which results in an increased resistance. Remarkably, the composite can be stretched further until breakage as the wt% of CB & CNTs increases. The composite with 15 wt% filler had an extensibility of 125% while the composite with 6 wt% filler broke at a relative elongation of 70%.

Out of the four samples, the sample with 9 wt% filler was the only sample that did not gain a notable increase in resistance compared to the original resistance, which is favorable for stretchable conductors. On the other hand, the sample with 6 wt% filler exhibited the highest gauge factor, making it an interesting candidate for a strain sensor. However, the initial resistances (k**Ω**) are still too high in order to use the specimens as stretchable conductors.

3.4.2 Composite of multi-walled carbon nanotubes and PDMS

The resistance of the multi-walled carbon nanotube composite is dependent of the relative elongation of the sample, as shown in the following figure.

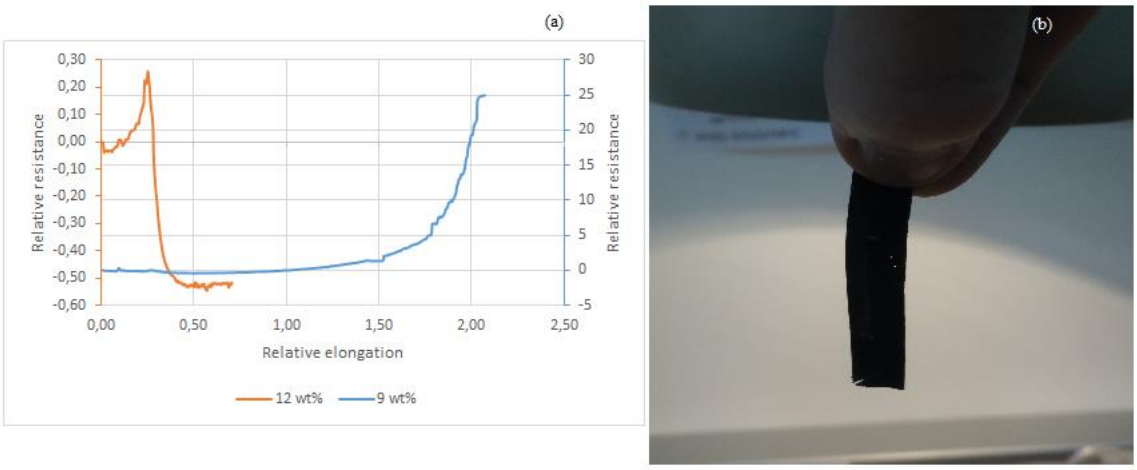

Figure 26: The relative resistance as a function of relative elongation of PDMS/ MWCNT composites (a) and the presence of small holes in the sample of 9 wt% filler (b)

A remarkable difference between both samples can be observed. The specimen of 9 wt% filler broke at a relative elongation of 205% while the other specimens broke at a relative elongation of 70%. This is explained by the presence of small holes in the sample of 9 wt% filler due to the improper removal of air bubbles, as depicted in the figure (above). The small holes and the rough edges produced by laser cutting aggravated the mechanical properties of the sample.

However, the specimen of 9 wt% MWCNTs exhibited interesting properties. While the relative elongation was under 100%, the resistance remained almost constant. The relative resistance rose quickly at a relative elongation of 170%. This behavior is ideal for stretchable electronics but unfortunately, the initial resistance of 196 k**Ω** is too high.

3.4.3 Composite of Matrix and PDMS

The results of the tensile tests for the composites of PDMS and Matrix are shown in the following figure.

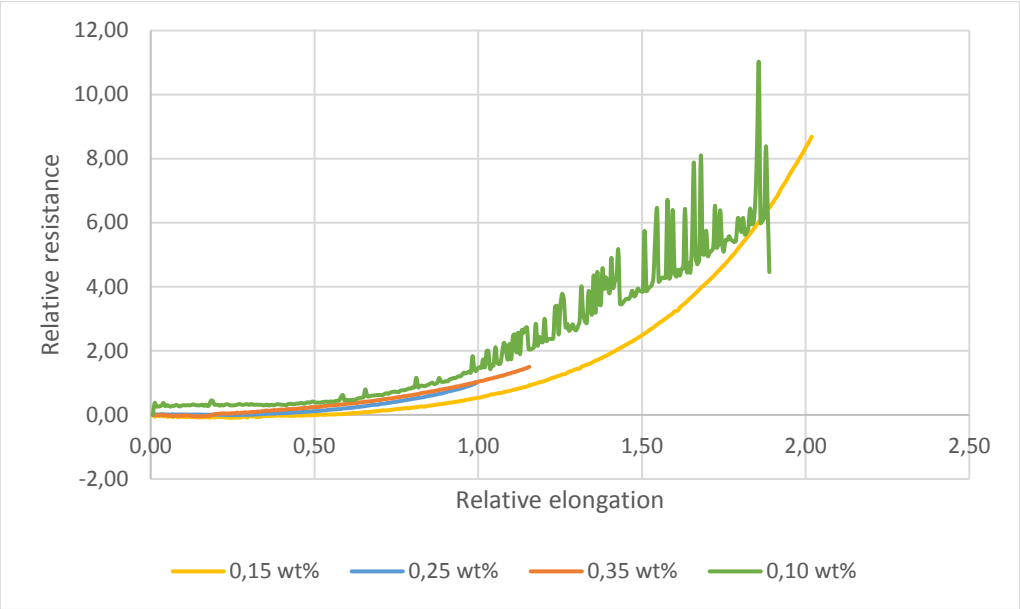

Figure 27: The relative resistance as a function of relative elongation of PDMS/ Matrix composites

The first thing that stands out is the noise on the sample of 0.10 wt% Matrix. This can be explained due to improper clamping of the sample. When the sample elongates, it becomes thinner and the grip on the sample decreases which causes occasional bad contact between the sample and the copper tape.

Although noise is present on the sample of 0.10 wt% Matrix, the behavior under strain is similar to the other samples. The resistance of each sample increases gradually until breakage. It is important to notice that the samples with a higher amount of filler exhibit a lower extensibility than the samples with a lower filler amount, which is the opposite behavior of the PDMS/ CB & CNTs composites.

3.4.4 Composite of Pristine single-walled carbon nanotubes and PDMS

During the measurement of the sample with 0.10 wt% SWCNTs, constant contact losses occurred, making the results unusable. Therefore, only the results of the sample with 0.15 wt% SWCNTs are reported.

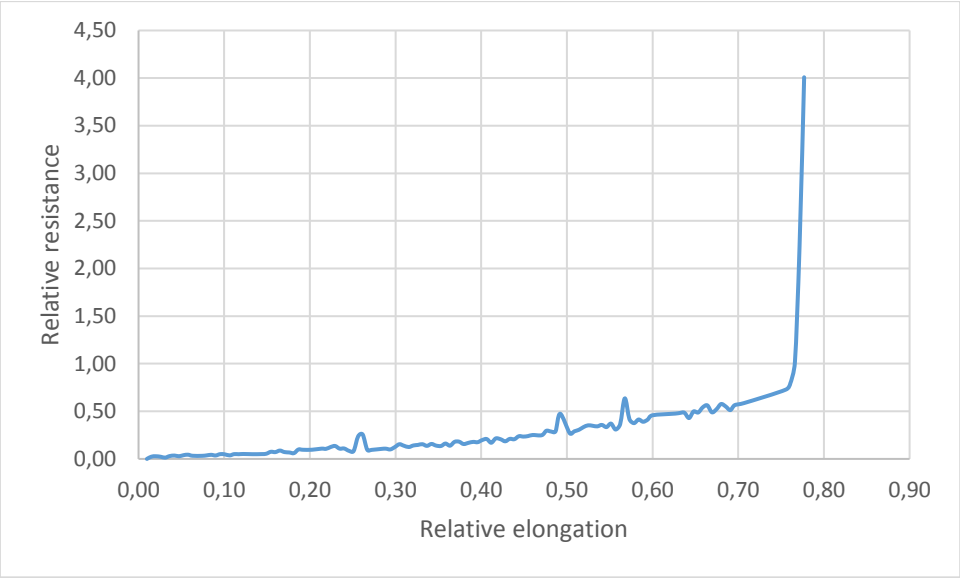

Figure 28: The relative resistance as a function of relative elongation of a PDMS/ SWCNTs composite

Until an elongation of 70%, the change in relative resistance of the pristine SWCNTs composite is comparable with the change in relative resistance of the Matrix composite (0.15 wt% Matrix). However, at an elongation of 76%, the resistances increases drastically and the sample breaks. This can be explained due to the presence of a rough edges which is created during laser cutting.

4. Discussion and conclusion

The main goal of this thesis was to survey the percolation threshold of multiple conductive particles in a silicone matrix. Furthermore, the effect of elongation on the resistance of the composite is determined. The added value lies in the accuracy and reproducibility of the composites. Additionally, the mapping of the percolation thresholds allows the researcher to estimate the amount of conductive filler which needs to be added in order to make the composite conductive.

The literature review at the start of this thesis gave insight in the design of conductive composites. Firstly, key characteristics of the reported percolation thresholds were analyzed, such as the aspect ratio of the used fillers, in order to estimate the threshold of the used fillers in this thesis. Secondly, multiple dispersion techniques were investigated, based on the availability of machines and facilities of the lab.

After the initial literature study, the dispersion methods of choice were familiarized by performing experiments with low-end fillers. This ensured proper usage of the more expensive fillers. After fine-tuning the dispersion methods, three roll milling and high speed mixing yielded the best dispersion quality. Afterwards, the percolation threshold of each high-end filler could be determined. The following table gives an overview of the achieved percolation thresholds.

Table 26: Comparison of the achieved percolation thresholds of the fillers

Filler	Volume percentage (vol%)	Weight percentage (wt%)	Resistance (**Ω**)
CB & CNTs	29.22	6	7.50×10^4
MWCNTs	5.34	9	1.32×10^6
SWCNTs in PDMS oil (Matrix)	0.09	0.10	2.24×10^7
Pristine SWCNTs	Incalculable (unknown pristine SWCNT density)	0.10	2.23×10^7

Although the percolation threshold was not reached in silver nanowires, carbon black and silver coated copper flakes, an interesting observation could be made. When the aspect ratio of the used filler increases, the percolation threshold decreases because of the higher entanglement of high aspect ratio fillers.

Additionally, the relation between the extensibility and resistance was determined by measuring the resistance while stretching. The characterization indicated that the presence of spherical particles increased the extensibility of the composite. Furthermore, the change in resistance of the composite is higher with the presence

of spherical particles than with carbon nanotubes. This indicates that composites containing spherical particles such as carbon black are suitable for strain gauge applications, while composites with carbon nanotubes exhibit favorable characteristics for stretchable circuits. However, the initial resistances are too high to in order to be used for stretchable circuits but the use of particles with a lower intrinsic resistance can increase the conductivity of the composite.

In conclusion, this Master's thesis determined the percolation threshold of four different conductive fillers and investigated the suitability of the composites for stretchable electronics. Recommendations for future work includes the use of a different elastomer such as Ecoflex which exhibits a higher intrinsic extensibility than PDMS. Next, the use of a hot press for curing the composites is advised since the particles are more densely packed, resulting in a higher entanglement of the particles. And finally, the combination of high speed mixing and three roll milling is possible improvement for the dispersion state of the filler. The high speed mixer is used in order to obtain a homogenous suspension, while the three roll mill is used to eliminate any remaining agglomerates.

Bibliography

[1] Z. Research, "Flexible Electronics Market Size Will Grow USD 16.50 billion by 2021: Zion Market Research", *GlobeNewswire News Room*, 2017. [Online]. Available: https://globenewswire.com/news-release/2017/07/05/1038820/0/en/Stretchable-Electronics-Market-Size-Will-Grow-USD-16-50-billion-by-2021-Zion-Market-Research.html. [Accessed: 21- Oct- 2017].

[2] N. Medicine, "Stretchable Electronics in Health Technology | Northwestern Medicine", *Northwestern Medicine*, 2017. [Online]. Available: http://www.nmbreakthroughs.org/medical-advances/stretchable-health-technology. [Accessed: 21- Oct- 2017].

[3]J. Machiels, "In Situ Measurement of Percolation Threshold of Conductive Fillers and Integration into a Self-Healing Elastomer", Master, Uhasselt, KULeuven, 2017.

[4] M. Park, J. Park and U. Jeong, "Design of conductive composite elastomers for stretchable electronics", Nano Today, vol. 9, no. 2, pp. 244-260, 2014. [5] 2017. [Online]. Available: http://iopscience.iop.org/article/10.1088/1742-6596/439/1/012009/pdf. [Accessed: 21- Oct- 2017].

[6] O. MWCNTs (>95%, "MWCNTs (>95%, OD: 10-20 nm)", Us-nano.com, 2018. [Online]. Available: https://www.us-nano.com/inc/sdetail/224. [Accessed: 04- Jun- 2018].

[7] J. Yang and J. Liang, "A modified model of electrical conduction for carbon black-polymer composites", Polymer International, vol. 60, no. 5, pp. 738-742, 2011.

[8] X. Liang, T. Zhao, Y. Hu and R. Sun, "Dielectric properties of silver nanowires-filled polyvinylidene fluoride composite with low percolation threshold", Journal of Nanoparticle Research, vol. 16, no. 9, 2014. [65] Metallpulver24.de. (2017). Kupferpulver eConduct 50g Dose (590,-€ / 1kg) - Metallpulver & Granulate. [online] Available at: https://www.metallpulver24.de/de/kupferpulver-econduct-50g-dose.html [Accessed 21 Oct. 2017].

[9] "Kupferpulver eConduct" [Online]. Available: https://www.metallpulver24.de/de/kupferpulver-econduct-50g-dose.html. [Accessed: 21- Oct- 2017].

[12] Axisa and Brosteaux, "BIOMEDICAL STRETCHABLE SYTEMS USING MID BASED STRETCHABLE ELECTRONICS TECHNOLOGY", 2007.

[13] M. Gonzalez, F. Axisa, M. Bulcke, D. Brosteaux, B. Vandevelde and J. Vanfleteren, "Design of metal interconnects for stretchable electronic circuits", Microelectronics Reliability, vol. 48, no. 6, pp. 825-832, 2008.

[14] R. Mutiso, "Electrical Percolation In Metal Nanowire Networks For Bulk Polymer Nanocomposites And Transparent Conductors, And Resistive Switching In Metal/polymer Nano-Gap Devices and an Unsaturated Polyester Resin", PhD, 2013.

[15] "Critical volume fractions in conductive composites", Composites, vol. 24, no. 7, p. 593, 1993.

[16]]N. Hush, "Electron tunnelling in chemistry: chemical reactions over large distances", Journal of Electroanalytical Chemistry and Interfacial Electrochemistry, vol. 309, no. 1-2, pp. 365-366, 1991.

[17] I. Balberg, "A comprehensive picture of the electrical phenomena in carbon black–polymer composites", Carbon, vol. 40, no. 2, pp. 139-143, 2002.

[18] http://shodhganga.inflibnet.ac.in/bitstream/10603/129893/10/10_chapter%202.pdf. [Online]. Available: http://shodhganga.inflibnet.ac.in/bitstream/10603/129893/10/10_chapter%202.pdf. [Accessed: 04- Jun- 2018].

[19] G. Kaur, R. Adhikari, P. Cass, M. Bown and P. Gunatillake, "Electrically conductive polymers and composites for biomedical applications", RSC Advances, vol. 5, no. 47, pp. 37553-37567, 2015.

[20] Berhan, L.; Sastry, A., Modeling Percolation in High-Aspect-Ratio Fiber Systems. I. Soft-Core Versus Hard-Core Models. Physical Review E 2007, 75.

[21] D. Stroud, "The effective medium approximations: Some recent developments", Superlattices and Microstructures, vol. 23, no. 3-4, pp. 567-573, 1998.

[22] I. Rosca and S. Hoa, "Highly conductive multiwall carbon nanotube and epoxy composites produced by three-roll milling", Carbon, vol. 47, no. 8, pp. 1958-1968, 2009. conductive multiwall carbon nanotube and epoxy composites produced by three-roll milling

[23] X. Huang and C. Zhi, Polymer nanocomposites.

[24] Q. Xue, "The influence of particle shape and size on electric conductivity of metal–polymer composites", European Polymer Journal, vol. 40, no. 2, pp. 323-327, 2004.

[25] X. Jing, "Effect of particle size on electric conducting percolation threshold in polymer/conducting particle composites", 2018.

[26] K. Kalaitzidou, H. Fukushima and L. Drzal, "A Route for Polymer Nanocomposites with Engineered Electrical Conductivity and Percolation Threshold", Materials, vol. 3, no. 2, pp. 1089-1103, 2010.

[27] Y. Zheng, Y. Li, Z. Li, Y. Wang, K. Dai, G. Zheng, C. Liu and C. Shen, "The effect of filler dimensionality on the electromechanical performance of polydimethylsiloxane based conductive nanocomposites for flexible strain sensors", Composites Science and Technology, vol. 139, pp. 64-73, 2017.

[28] [C. Wu, H. Lin, J. Hsu, M. Yip and W. Fang, "Static and dynamic mechanical properties of polydimethylsiloxane/carbon nanotube nanocomposites", Thin Solid Films, vol. 517, no. 17, pp. 4895-4901, 2009.

[29] R. Ramalingame, P. Chandraker and O. Kanoun, "Investigation on the Influence of Solvents on MWCNT-PDMS Nanocomposite Pressure Sensitive Films", Proceedings, vol. 1, no. 4, p. 384, 2017.

[30] C. Liu and J. Choi, "Improved Dispersion of Carbon Nanotubes in Polymers at High Concentrations", Nanomaterials, vol. 2, no. 4, pp. 329-347, 2012.

[31]C. Lee, L. Jug and E. Meng, "High strain biocompatible polydimethylsiloxane-based conductive graphene and multiwalled carbon nanotube nanocomposite strain sensors", Applied Physics Letters, vol. 102, no. 18, p. 183511, 2013.

[32] S. Hassouneh, L. Yu, A. Skov and A. Daugaard, "Soft and flexible conductive PDMS/MWCNT composites", Journal of Applied Polymer Science, vol. 134, no. 18, 2017.

[33] J. Li, P. Ma, W. Chow, C. To, B. Tang and J. Kim, "Correlations between Percolation Threshold, Dispersion State, and Aspect Ratio of Carbon Nanotubes", Advanced Functional Materials, vol. 17, no. 16, pp. 3207-3215, 2007.

[34] M. Atieh, N. Girun, E. Mahdi, H. Tahir, C. Guan, M. Alkhatib, F. Ahmadun and D. Baik, "Effect of Multi-Wall Carbon Nanotubes on the Mechanical Properties of Natural Rubber", Fullerenes, Nanotubes and Carbon Nanostructures, vol. 14, no. 4, pp. 641-649, 2006.

[35] Y. Huang and E. Terentjev, "Dispersion and rheology of carbon nanotubes in polymers", International Journal of Material Forming, vol. 1, no. 2, pp. 63-74, 2008.

[36] "Sonication of Biosolids — SONOTRONIC", Sonotronic.de, 2018. [Online]. Available: https://sonotronic.de/technologies/ultrasonic/sonication-of-bio-solids. [Accessed: 04- Jun- 2018].

[37] L. Dumée, K. Sears, J. Schütz, N. Finn, M. Duke and S. Gray, "Influence of the Sonication Temperature on the Debundling Kinetics of Carbon Nanotubes in Propan-2-ol", Nanomaterials, vol. 3, no. 1, pp. 70-85, 2013.

[38] F. Delogu, G. Gorrasi and A. Sorrentino, "Fabrication of polymer nanocomposites via ball milling: Present status and future perspectives", Progress in Materials Science, vol. 86, pp. 75-126, 2017.

[39] Y. Tang, N. Witt and L. Ye, "Conductive Rubber Nanocomposites as Tensile and Pressure Sensors", Applied Mechanics and Materials, vol. 217-219, pp. 130-133, 2012.

[40] N. Witt, Y. Tang, L. Ye and L. Fang, "Silicone rubber nanocomposites containing a small amount of hybrid fillers with enhanced electrical sensitivity", Materials & Design, vol. 45, pp. 548-554, 2013.

[41] N. Pierard, A. Fonseca, J. Colomer, C. Bossuot, J. Benoit, G. Van Tendeloo, J. Pirard and J. Nagy, "Ball milling effect on the structure of single-wall carbon nanotubes", Carbon, vol. 42, no. 8-9, pp. 1691-1697, 2004.

[42] F. Bensadoun, N. Kchit, C. Billotte, F. Trochu and E. Ruiz, "A Comparative Study of Dispersion Techniques for Nanocomposite Made with Nanoclays and an Unsaturated Polyester Resin", Journal of Nanomaterials, vol. 2011, pp. 1-12, 2011.

[43] J. Ruhhammer, M. Zens, F. Goldschmidtboeing, A. Seifert and P. Woias, "Highly elastic conductive polymeric MEMS", Science and Technology of Advanced Materials, vol. 16, no. 1, p. 015003, 2015.

[44] S. Stassi, G. Canavese, F. Cosiansi, R. Gazia and M. Cocuzza, "A Tactile Sensor Device Exploiting the Tunable Sensitivity of Copper-PDMS Piezoresistive Composite", Procedia Engineering, vol. 47, pp. 659-663, 2012.

[45] Y. Dong, R. Umer and A. Lau, Fillers and reinforcements for advanced nanocomposites. p. 351.

[46] "Three roll mills | Thicol Boya Makina Sanayi", Thicol Boya Makina Sanayi, 2018. [Online]. Available: http://www.thicolmakina.com/en/products/paint-grinding-machines/. [Accessed: 04- Jun- 2018].

[47] "Home of the Other Three Roll Mill Manufacturer", Threerollmill.com, 2018. [Online]. Available: http://www.threerollmill.com/. [Accessed: 04- Jun- 2018].

[48] M. Loos, Carbon nanotube reinforced composites. p. 185.

[49] M. Raza, A. Westwood and C. Stirling, "Carbon black/graphite nanoplatelet/rubbery epoxy hybrid composites for thermal interface applications", Journal of Materials Science, vol. 47, no. 2, pp. 1059-1070, 2011.

[50] Gang Yin, Ning Hu, Y. Karube, Yaolu Liu, Yuan Li and H. Fukunaga, "A carbon nanotube/polymer strain sensor with linear and anti-symmetric piezoresistivity", Journal of Composite Materials, vol. 45, no. 12, pp. 1315-1323, 2011.

[51] Y. Dong, R. Umer and A. Lau, Fillers and reinforcements for advanced nanocomposites. p. 351.

[52] K. Sadasivuni, D. Ponnamma, J. Cabibihan and M. AlMa'adeed, "Electronic Applications of Polydimethylsiloxane and Its Composites", 2018. .

[53] R. Morent, N. De Geyter, F. Axisa, N. De Smet, L. Gengembre, E. De Leersnyder, C. Leys, J. Vanfleteren, M. Rymarczyk-Machal, E. Schacht and E. Payen, "Adhesion enhancement by a dielectric barrier discharge of PDMS used for flexible and stretchable electronics", Journal of Physics D: Applied Physics, vol. 40, no. 23, pp. 7392-7401, 2007.

[54] "Single, Double, MultiWall Carbon Nanotube Properties & Applications", Sigma-Aldrich, 2018. [Online]. Available: https://www.sigmaaldrich.com/technical-documents/articles/materials-science/single-double-multi-walled-carbon-nanotubes.html. [Accessed: 04- Jun- 2018].

[55] OM. Fayemiwo, "BTEX compounds in water - future trends and directions for water treatment", 2017.

[56] B. Kiss-Pataki, "STUDY OF CARBON NANOTUBE FILLER DISPERSION IN POLYMER COMPOSITES BY VARIOUS MICROSCOPIC METHODS", 2015.

[57] J. Kim, J. Hwang, H. Hwang, H. Kim, J. Lee, J. Seo, U. Shin and S. Lee, "Simple and cost-effective method of highly conductive and elastic carbon

nanotube/polydimethylsiloxane composite for wearable electronics", Scientific Reports, vol. 8, no. 1, 2018.

[58] W. Bauhofer and J. Kovacs, "A review and analysis of electrical percolation in carbon nanotube polymer composites", Composites Science and Technology, vol. 69, no. 10, pp. 1486-1498, 2009.

[59] J. Benoit, B. Corraze, S. Lefrant, W. Blau, P. Bernier and O. Chauvet, "Transport properties of PMMA-Carbon Nanotubes composites", Synthetic Metals, vol. 121, no. 1-3, pp. 1215-1216, 2001.

[60] "Carbon nanotube, multi-walled 659258", Sigma-Aldrich, 2018. [Online]. Available: https://www.sigmaaldrich.com/catalog/product/aldrich/659258?lang=en&region=BE. [Accessed: 04- Jun- 2018].

[61] "OCSiAl", Ocsial.com, 2018. [Online]. Available: https://ocsial.com/en/material-solutions/tuball/. [Accessed: 04- Jun- 2018].

[62] "OCSiAl", Ocsial.com, 2018. [Online]. Available: https://ocsial.com/en/products/tuball-matrix-603/. [Accessed: 04- Jun- 2018].

[63] R. Rothon, Fillers for Polymer Applications. Springer Verlag, 2017.

[64] V. Jha, "Carbon Black Filler Reinforcement of Elastomers", PhD, 2008.

[65] E. Kanhere, M. Bora, J. Miao and M. Triantafyllou, "Flexible Hydrogel Capacitive Pressure Sensor for Underwater Applications", Proceedings, vol. 1, no. 4, p. 360, 2017.

[66] S. Powder, "Super Adsorption Activated Porous Carbon Powder", Us-nano.com, 2018. [Online]. Available: https://www.us-nano.com/inc/sdetail/32769. [Accessed: 04- Jun- 2018].

[67] Y. Zheng, Y. Li, K. Dai, Y. Wang, G. Zheng, C. Liu and C. Shen, "A highly stretchable and stable strain sensor based on hybrid carbon nanofillers/polydimethylsiloxane conductive composites for large human motions monitoring", Composites Science and Technology, vol. 156, pp. 276-286, 2018.

[68] S. Mixed, "Super Conductive Carbon Black Nanopowder and Carbon Nanotube Mixed", Us-nano.com, 2018. [Online]. Available: https://www.us-nano.com/inc/sdetail/4509. [Accessed: 04- Jun- 2018].

[69] A. Kelley, R. Cahn and M. Bever, Concise encyclopedia of composite materials. Oxford: Pergamon, 1995, p. 355. [70] Production of silver-coated copper-based powders US5178909A

[71] H. Chuang and S. Wereley, "Design, fabrication and characterization of a conducting PDMS for microheaters and temperature sensors", Journal of Micromechanics and Microengineering, vol. 19, no. 4, p. 045010, 2009. [72] https://www.eckart.net/uploads/tx_driveeckartproducts/EE-010359.pdf

[73] P. Zhang, I. Wyman, J. Hu, S. Lin, Z. Zhong, Y. Tu, Z. Huang and Y. Wei, "Silver nanowires: Synthesis technologies, growth mechanism and multifunctional applications", Materials Science and Engineering: B, vol. 223, pp. 1-23, 2017.

[74] F. Xu and Y. Zhu, "Highly Conductive and Stretchable Silver Nanowire Conductors", Advanced Materials, vol. 24, no. 37, pp. 5117-5122, 2012.

[75] J. Kim, J. Park, U. Jeong and J. Park, "Silver nanowire network embedded in polydimethylsiloxane as stretchable, transparent, and conductive substrates", Journal of Applied Polymer Science, vol. 133, no. 33, 2016.

[76] H. Liu, B. Pan and G. Liou, "Highly transparent AgNW/PDMS stretchable electrodes for elastomeric electrochromic devices", Nanoscale, vol. 9, no. 7, pp. 2633-2639, 2017.

[77] Z. Yu, Q. Zhang, L. Li, Q. Chen, X. Niu, J. Liu and Q. Pei, "Highly Flexible Silver Nanowire Electrodes for Shape-Memory Polymer Light-Emitting Diodes", Advanced Materials, vol. 23, no. 5, pp. 664-668, 2010.

[78] H. Cui, J. Jiu, K. Suganuma and H. Uchida, "Super flexible, highly conductive electrical compositor hybridized from polyvinyl alcohol and silver nano wires", RSC Advances, vol. 5, no. 10, pp. 7200-7207, 2015.

[79] X. Liang, T. Zhao, Y. Hu and R. Sun, "Dielectric properties of silver nanowires-filled polyvinylidene fluoride composite with low percolation threshold", Journal of Nanoparticle Research, vol. 16, no. 9, 2014.

[80] A. Lonjon, P. Demont, E. Dantras and C. Lacabanne, "Low filled conductive P(VDF-TrFE) composites: Influence of silver particles aspect ratio on percolation threshold from spheres to nanowires", Journal of Non-Crystalline Solids, vol. 358, no. 23, pp. 3074-3078, 2012.

[81] "Silver nanowires 739421", Sigma-Aldrich, 2018. [Online]. Available: https://www.sigmaaldrich.com/catalog/product/aldrich/739421?lang=en&region=BE. [Accessed: 04- Jun- 2018].

[82] B. Marinho, M. Ghislandi, E. Tkalya, C. Koning and G. de With, "Electrical conductivity of compacts of graphene, multi-wall carbon nanotubes, carbon black, and graphite powder", Powder Technology, vol. 221, pp. 351-358, 2012.

[83] "Resistance and Resistivity", Hyperphysics.phy-astr.gsu.edu, 2018. [Online]. Available: http://hyperphysics.phy-astr.gsu.edu/hbase/electric/resis.html. [Accessed: 04- Jun- 2018].

[84] S. Ganguli, A. Roy and D. Anderson, "Improved thermal conductivity for chemically functionalized exfoliated graphite/epoxy composites", Carbon, vol. 46, no. 5, pp. 806-817, 2008.

[85] M. García, J. Marchese and N. Ochoa, "Effect of the particle size and particle agglomeration on composite membrane performance", Journal of Applied Polymer Science, p. n/a-n/a, 2010.

[86] M. Safdari and M. Al-Haik, "Synergistic electrical and thermal transport properties of hybrid polymeric nanocomposites based on carbon nanotubes and graphite nanoplatelets", Carbon, vol. 64, pp. 111-121, 2013.

[87]]M. Loadman, Analysis of rubber and rubber-like polymers. [Place of publication not identified]: Springer, 2013, p. 115.

Auteursrechtelijke overeenkomst

Ik/wij verlenen het wereldwijde auteursrecht voor de ingediende eindverhandeling:
A study on the state of the art of conductive silicone nanocomposites for stretchable electronics

Richting: **master in de industriële wetenschappen: elektronica-ICT**
Jaar: **2018**

in alle mogelijke mediaformaten, - bestaande en in de toekomst te ontwikkelen - , aan de Universiteit Hasselt.

Niet tegenstaand deze toekenning van het auteursrecht aan de Universiteit Hasselt behoud ik als auteur het recht om de eindverhandeling, - in zijn geheel of gedeeltelijk -, vrij te reproduceren, (her)publiceren of distribueren zonder de toelating te moeten verkrijgen van de Universiteit Hasselt.

Ik bevestig dat de eindverhandeling mijn origineel werk is, en dat ik het recht heb om de rechten te verlenen die in deze overeenkomst worden beschreven. Ik verklaar tevens dat de eindverhandeling, naar mijn weten, het auteursrecht van anderen niet overtreedt.

Ik verklaar tevens dat ik voor het materiaal in de eindverhandeling dat beschermd wordt door het auteursrecht, de nodige toelatingen heb verkregen zodat ik deze ook aan de Universiteit Hasselt kan overdragen en dat dit duidelijk in de tekst en inhoud van de eindverhandeling werd genotificeerd.

Universiteit Hasselt zal mij als auteur(s) van de eindverhandeling identificeren en zal geen wijzigingen aanbrengen aan de eindverhandeling, uitgezonderd deze toegelaten door deze overeenkomst.

Voor akkoord,

Rutten, Jeff

Datum: **5/06/2018**